

# Lawrence Berkeley National Laboratory

## LBL Publications

### Title

Liquid Hydrogen Bubble Chambers

### Permalink

<https://escholarship.org/uc/item/7xq780vr>

### Authors

Dittler, Harry Cline

Gerecke, Thomas Frank

### Publication Date

1955-05-01

UCRL 2985  
cy 2

UNIVERSITY OF  
CALIFORNIA

*Radiation  
Laboratory*

BERKELEY, CALIFORNIA

## **DISCLAIMER**

This document was prepared as an account of work sponsored by the United States Government. While this document is believed to contain correct information, neither the United States Government nor any agency thereof, nor the Regents of the University of California, nor any of their employees, makes any warranty, express or implied, or assumes any legal responsibility for the accuracy, completeness, or usefulness of any information, apparatus, product, or process disclosed, or represents that its use would not infringe privately owned rights. Reference herein to any specific commercial product, process, or service by its trade name, trademark, manufacturer, or otherwise, does not necessarily constitute or imply its endorsement, recommendation, or favoring by the United States Government or any agency thereof, or the Regents of the University of California. The views and opinions of authors expressed herein do not necessarily state or reflect those of the United States Government or any agency thereof or the Regents of the University of California.

UCRL-2985  
Unclassified Physics

UNIVERSITY OF CALIFORNIA

Radiation Laboratory  
Berkeley, California

Contract No. W-7405-eng-48

LIQUID HYDROGEN BUBBLE CHAMBERS

Harry Cline Dittler and Thomas Frank Gerecke

(M.S. Thesis)

May 10, 1955

Submitted in partial fulfillment  
of the requirements for the degree of  
MASTER OF SCIENCE

in

PHYSICS

United States Naval Postgraduate School  
Monterey, California

Printed for the U. S. Atomic Energy Commission

LIQUID HYDROGEN BUBBLE CHAMBERS  
Harry Cline Dittler and Thomas Frank Gerecke  
Radiation Laboratory  
University of California, Berkeley, California

May 10, 1955

ABSTRACT

An ionizing particle, under the proper conditions, forms a string of bubbles along its path through a superheated liquid. Although spontaneous boiling in a chamber of glass-and-metal construction has limited the duration of superheat to approximately 50 milliseconds, the tracks of particles from a pulsed accelerator have been photographed with great success. The characteristics of a detector that utilizes this principle permit taking photographs with little or no background contamination at a frequency matching the pulse rate of Bevatron-Cosmotron type accelerators. A four-inch liquid hydrogen bubble chamber has been built and operated successfully in the beams of the Berkeley synchrocyclotron (184-inch cyclotron) and the Bevatron. This chamber and its associated control and instrumentation equipment are described in some detail. Basic theoretical considerations, advantages, preliminary physics experiments, and future developmental planning are also discussed.

## PREFACE

For the past eight months the authors have been working under Dr. Luis W. Alvarez in the Physics Research Division of the University of California Radiation Laboratory in Berkeley. During this period we have worked with the Bubble Chamber Group on the construction and testing of a four-inch liquid hydrogen bubble chamber. This chamber is now an operating reality and has been used for physics research in the beams of the Bevatron and the 184-inch cyclotron. It is now being used primarily for design studies in connection with the development of larger chambers planned for the near future. The four-inch chamber is, in a sense, the result of a group effort, but the mechanical details of its construction and operation are largely the result of work by Arnold J. Schwemin and Douglas Parmentier, Jr., of this laboratory.

For use with pulsed accelerators in the study of nuclear interactions, the bubble chamber possesses several distinct advantages over other detectors. These advantages include its relatively high density, leading to a higher probability of recording a desired event. Its high repetition rate and short sensitive time, make possible a large number of photographs with the interesting events unobscured by undesirable background. A liquid hydrogen bubble chamber possesses the added advantage of having essentially only protons in its sensitive volume.

It is the aim of this paper to present some of the theoretical and practical aspects of hydrogen bubble chambers in sufficient detail to adequately describe their operation.

We wish particularly to express our gratitude for the encouragement and suggestions of Dr. Luis W. Alvarez during the entire period of the work on this project. We also extend our thanks to Dr. M. Lynn Stevenson, Dr. Frank S. Crawford, Jr., J. Donald Gow and Harrold B. Knowles for their informative discussions and criticisms of this paper. We are grateful for the help given by Richard L. Blumberg, Arnold J. Schwemin, and Douglas Parmentier, Jr. on the mechanical details of the chamber, and by Vern G. Ogren and John J. Barale on the electronics. We further wish to thank Dr. Roderick K. Clayton of the U. S. Naval Postgraduate School, who reviewed the completed paper and offered many constructive criticisms. We are indebted to Dr. Donald A. Glaser and Dr. Roger H. Hildebrand for providing photographs of their early chambers and to the Technical Information Division of the University of California Radiation Laboratory for their cheerful cooperation in the final preparation and printing of this paper.

This work was done under the joint auspices of the United States Naval Postgraduate School and the United States Atomic Energy Commission.

## TABLE OF CONTENTS

Item	Title	Page
Chapter I	Introduction . . . . .	1
	1. Historical Background . . . . .	1
	2. Summary . . . . .	5
Chapter II	Thermodynamics . . . . .	7
	1. Thermal Properties of Real Gases . . . . .	7
	2. The Equation of State for Hydrogen . . . . .	9
	3. Qualitative Analysis of the Thermodynamic Cycle . . . . .	14
Chapter III	Bubble Formation and Growth . . . . .	16
	1. Nucleation . . . . .	16
	2. Bubble Growth . . . . .	16
	3. Experimental Results . . . . .	21
Chapter IV	Construction and Operation . . . . .	23
	1. Construction Features . . . . .	23
	2. Preparations for Operation . . . . .	30
	3. Operation . . . . .	33
	4. Adjustment of Operating Conditions . . . . .	34
Chapter V	Control and Instrumentation . . . . .	37
	1. General . . . . .	37
	2. Timing Circuit . . . . .	37
	3. Chamber Temperature . . . . .	40
	4. Pressure Measurement . . . . .	42
	5. Miscellaneous . . . . .	45
Chapter VI	Physics Experiments . . . . .	47
	1. Purpose . . . . .	47
	2. The 184-inch Cyclotron Experiment . . . . .	47
	3. The Bevatron Experiment . . . . .	47

Item	Title	Page
Chapter VII	Future Developments . . . . .	54
	1. General . . . . .	54
	2. The Four-inch Chamber . . . . .	54
	3. The Ten-inch Chamber . . . . .	55
	4. The Fifty-inch Chamber . . . . .	56
	5. Data Compilation and Analysis . . . . .	57
Chapter VIII	Advantages and Conclusions . . . . .	59
	1. General . . . . .	59
	2. Cloud Chambers . . . . .	59
	3. Nuclear Emulsions . . . . .	61
	4. Counters . . . . .	63
	5. Conclusions . . . . .	64
Bibliography . . . . .		65
Alphabetical Author List . . . . .		67

## LIST OF ILLUSTRATIONS

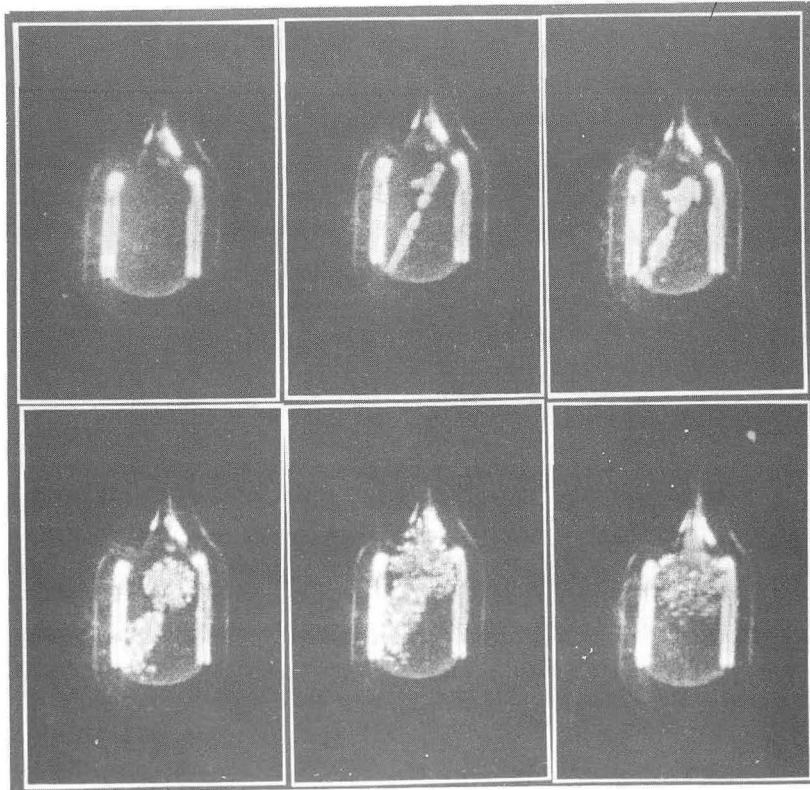
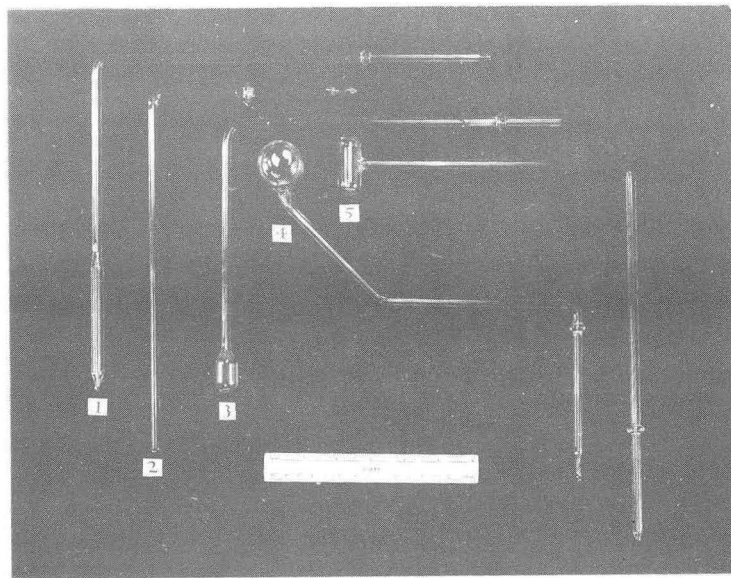
Figure	Page
1.	a. Glass Parts of Some of Glaser's Early Chambers . . . . . 2
	b. First Recorded Bubble Chamber Track . . . . . 2
2.	First Liquid Hydrogen Bubble Chamber by Hildebrand and Nagle . . . . . 4
3.	Pressure-Volume Plot for a Real Gas . . . . . 8
4.	Plot of the Reduced van der Waals Equation . . . . . 11
5.	Plot of the Virial Coefficients for Hydrogen . . . . . 12
6.	Comparison Plot of the van der Waals Equation and the Onnes Equation . . . . . 13
7.	Equilibrium Curves for Bubbles of Small Radius . . . . . 18
8.	Plot of Bubble Growth Rate in Liquid Hydrogen . . . . . 23
9.	Four-inch Liquid Hydrogen Bubble Chamber:Photographs 25
10.	Four-inch Liquid Hydrogen Bubble Chamber: Schematic Diagram . . . . . 26
11.	a. Glass-to-Metal Seals:Schematic Diagram . . . . . 29
	b. Photographic and Illumination Arrangement: Schematic Diagram . . . . . 29
12.	Timing Circuit:Block Diagram . . . . . 38
13.	Temperature-Measuring Arrangement:Schematic Diagram . . . . . 41
14.	Pressure-Measuring Circuit:Block Diagram . . . . . 43
15.	$\pi - \mu -$ electron Decay . . . . . 48
16.	$\pi^- - p^+$ Elastic Scattering . . . . . 50
17.	Decay of a V-Particle:Stereoscopic View . . . . . 51
18.	Creation and Decay of a V-Particle . . . . . 52
19.	$\pi$ -Meson Pair Production:Stereoscopic View . . . . . 53
20.	Biasing-out of Minimum Ionizing Particles . . . . . 62

## CHAPTER I INTRODUCTION

### 1. Historical Background.

The bubble chamber was invented by Dr. Donald A. Glaser (1, 2) at the University of Michigan. Although liquefied gases had been previously suggested as detecting media for cosmic rays (3), it was not until Dr. Glaser constructed and operated his ether bubble chamber in 1953 that the detecting possibilities of superheated liquids were utilized for this purpose. His first chamber consisted of a small, thick-walled, pyrex glass tube filled with diethyl ether. The liquid was heated to approximately  $130^{\circ}\text{C}$  and pressurized to about 20 atmospheres. When the pressure was released, he found that the ether, in the absence of any external source of radiation, would remain in a superheated state for periods up to about 400 seconds, the average being about 68 seconds. If a small  $\text{Co}^{60}$  source was placed near the chamber, however, there were immediate eruptions in the liquid when the pressure was released. He was soon able to photograph the tracks caused by cosmic ray particles passing through the sensitive volume of the chamber. Figure 1 shows several of the first glass chambers used by Glaser, and a series of photographs of the first bubble chamber track to be recorded.

Dr. Roger H. Hildebrand and Dr. Darragh E. Nagle (4), at the University of Chicago, after duplicating Glaser's experiment with ether, constructed a bubble chamber using liquid hydrogen as the detecting medium. In this chamber the hydrogen pressure was suddenly reduced from almost four atmospheres to one atmosphere. Again it was found that the liquid would remain quiescent in a



ZN-1259

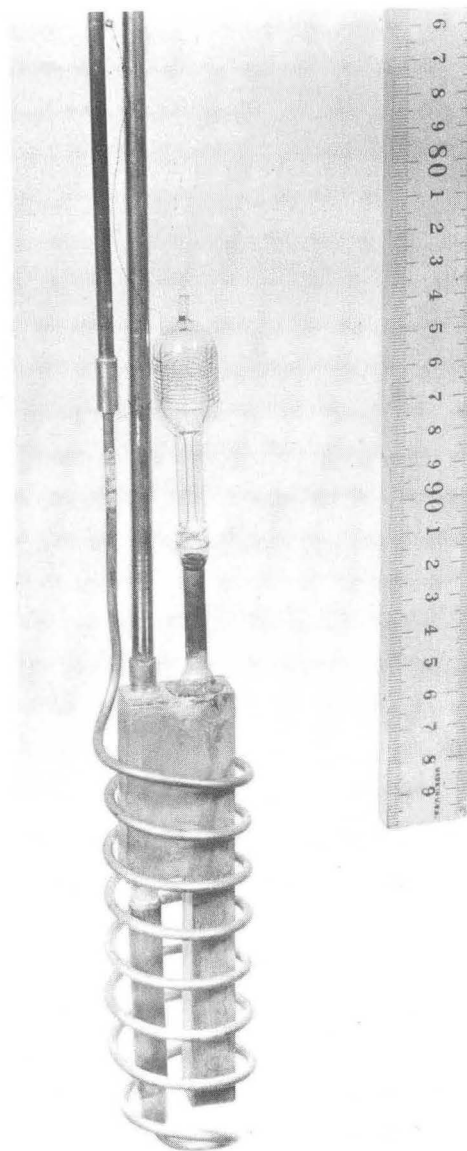
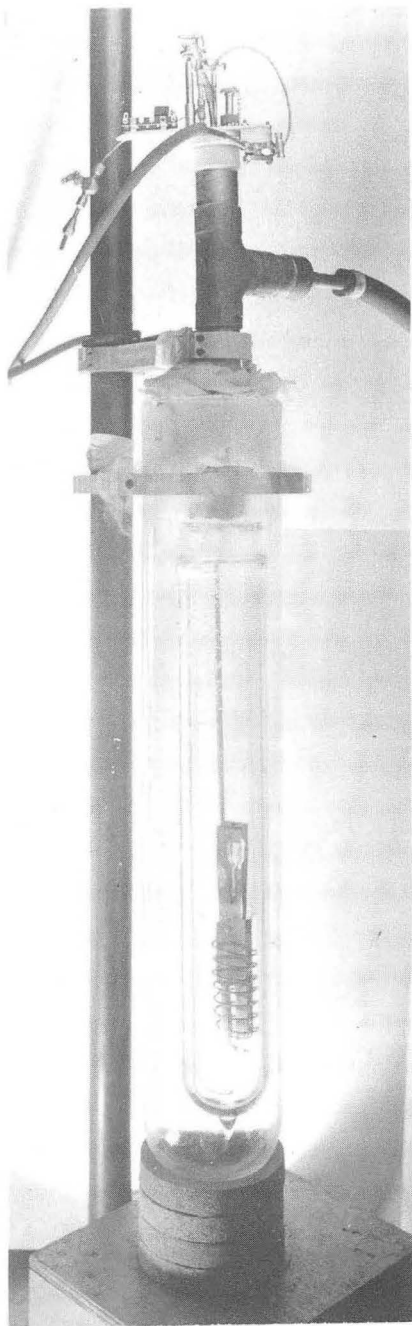
Fig. 1. (a) Glass parts of some of Glaser's early ether chambers. Nos. 1 and 2 were used to test the radiation sensitivity of liquids, No. 3 is typical of the first successful bubble chamber, and Nos. 4 and 5 are later models designed for specific applications. (b) Selected frames from a 3000-frame/second motion picture of the first recorded track. Times are 0, 1/3, 4, 20, 71, and 250 milliseconds. (Courtesy Donald A. Glaser).

superheated state for a considerable time if no external radiation were present, and that it would boil almost immediately in the presence of such radiation. This chamber was also constructed of pyrex glass. Figure 2 shows two views of the first successful liquid hydrogen bubble chamber operated by Hildebrand and Nagle.

At the University of California Radiation Laboratory, Dr. Luis W. Alvarez, after discussing the possible merits of bubble chambers with Glaser, considered that such a device filled with liquid hydrogen would be highly desirable for use with high-energy particle accelerators. Soon an ether chamber similar to Glaser's was constructed, and, by the end of 1953, a liquid hydrogen chamber had been completed and the first photographs made of tracks in liquid hydrogen (5). This chamber was also made entirely of glass. Soon another chamber was constructed that consisted essentially of a small brass cylinder with glass plates on each end for illumination and photography. It was surrounded by an outer cylinder or bath containing liquid hydrogen boiling at about 80 psig (pounds per square inch, gauge) to act as a heat reservoir and maintain a constant temperature in the chamber. The chamber was initially filled at a pressure slightly greater than 80 psig. The pressure was then suddenly reduced by opening the chamber to the atmosphere for a fraction of a second. Photographs of bubble tracks were obtained by using a synchronized stroboscopic lamp for illumination.

Although this chamber was constructed of metal and glass, it was found that operation could be sufficiently rapid so that bubbles formed on the metal surfaces and at the glass-to-metal seals did not have time to destroy the superheated state or to encroach into the active volume before the tracks were photographed.

The present four-inch chamber was designed for use with pulsed accelerators and was first operated late in 1954. Although



ZN-1260

Fig. 2. (a) Apparatus used by Hildebrand and Nagle in the first successful test of liquid hydrogen bubble chamber.

(b) Hildebrand's and Nagle's chamber with dewars and heat shield removed to allow a better view of bulb. (4)

(Courtesy Roger H. Hildebrand)

only a random distribution of bubbles could be obtained with nitrogen, tracks were obtained with hydrogen. It has been used successfully in the beams of both the 184-inch cyclotron and the Bevatron. Although it falls far short of the ultimate in bubble chamber design, it will be used as an example in this paper because it is the chamber with which the authors are most familiar, because it is the largest one built thus far, and because it does serve to illustrate the underlying theory and point out many of the problems to be encountered in future designs.

## 2. Summary.

If the pressure on a highly pressurized liquid is suddenly reduced, the liquid may become superheated. When an ionizing particle passes through a superheated liquid under the proper conditions, a string of bubbles is formed along its track, and these can be photographed to give a permanent record of the event. In a clean, smooth-walled vessel, and in the absence of any source of radiation, the superheated condition can be maintained for periods up to several hundred seconds. In a vessel of glass and metal construction, the period is reduced to the order of milliseconds. The spontaneous boiling, however, occurs only on the metal surfaces and at the glass-to-metal seals, and not on the smooth inner face of the glass ports. Tracks of particles from a pulsed accelerator can be created and photographed before this surface boiling encroaches very far into the sensitive volume of the chamber or reduces the superheat below the threshold value required for track formation. The bubbles appear to grow in radius approximately as the square root of the time, and so, by a judicious choice of the time delay between the passage of the particles and exposure of the photograph, pictures of clear, well-defined bubbles can be obtained. The density of bubbles along this track gives a measure of the ionizing power of

the particle. The curvature of this track in the presence of a magnetic field would give the signs and permit measuring the momenta of particles.

The chamber and associated equipment discussed in this paper were designed to operate in the beam from the Bevatron. The liquid in the chamber is kept at about 80 psig and 29° K until expansion. A few milliseconds before the arrival of the Bevatron pulse the pressure is reduced to just slightly over one atmosphere. A few milliseconds after the passage of the beam a light is flashed and the photograph is taken. An electronic timing circuit controls both the time of pressure release and the time of the photograph with respect to the beam time. The actual timing delays and the picture of the pressure variation during the cycle are presented on oscilloscopes.

## CHAPTER II

### THERMODYNAMICS

#### 1. Thermal Properties of Real Gases.

Basic thermodynamic theory incorporates the concept of an ideal gas, defined by the ideal equation of state,

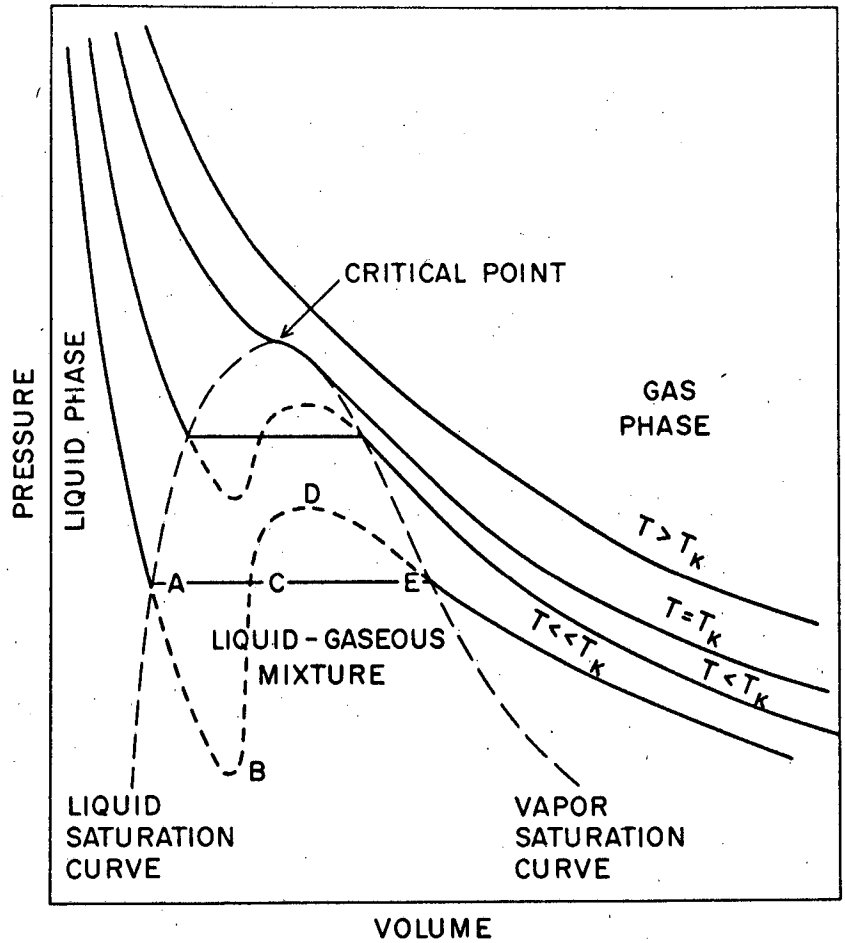
$$PV = nRT,$$

which results from a combination of Boyle's and Charles's laws. This simple equation holds well for actual gases at relatively high temperatures, but at temperatures approaching possible liquefaction, the equation no longer agrees with experimental observations.

It is an experimental fact that if a mass of any gas is kept at a constant temperature as the pressure is increased, the volume decreases. Figure 3 is a plot of some representative isotherms for a real gas and shows in more detail the manner in which the isothermal curves become complicated at lower temperatures where liquefaction occurs. No real gas behaves under all conditions like an ideal gas.

Let us examine Fig. 3 more closely. The maximum temperature at which a liquid and its saturated vapor can coexist in equilibrium is defined as the critical temperature. If a mass of gas at a temperature less than critical is compressed isothermally, slowly and with care, the values of pressure and volume can be made to vary in a manner represented by the line ED and we have a condition called supersaturation. This is an unstable state, and if compression is continued liquefaction occurs and the equilibrium point suddenly shifts to the straight line EC where the gas and liquid coexist in stable equilibrium.

Similarly, if a mass of liquid at a temperature less than critical is expanded isothermally, the values of pressure and volume can be



MU-9461

Fig. 3. A pressure-volume plot of representative isothermal curves for a real gas.

made to vary in a manner represented by the line AB if we adhere to rigid experimental conditions. The line ABC represents the condition where we have superheated liquid -- an unstable state. For this reason, a disturbance while the liquid is in this condition results in instantaneous boiling and subsequent return to the straight line AC where the liquid and gas coexist in stable equilibrium. This region in which we can have superheated liquid is of particular interest, because it is this phenomenon of "triggered" boiling that makes bubble chambers possible.

## 2. The Equation of State for Hydrogen.

Thomson in 1871 made the suggestion that the behavior of a real gas should be represented by a continuous curve similar to ABCDE. J. D. van der Waals subsequently developed his equation in 1877, which is

$$(P + a/V^2)(V - b) = RT,$$

or in powers of V,

$$V^3 - \frac{(Pb + RT)}{P} V^2 + \frac{a}{P} V - \frac{ab}{P} = 0,$$

which has three real roots below the critical temperature.

The physical interpretation of the modifying terms can be very simply explained. The term  $a/V^2$  is the cohesive pressure. This takes into account the fact that the molecules of gas at the surface of any containing vessel do not exert their full force on the surface; they are experiencing a force away from the surface due to the attraction of the rest of the gas.

The term  $b$  takes account of the actual volume of the gas molecules themselves. Thus the true volume is the apparent volume minus a constant term which represents the minimum possible volume of packing for the gas molecules.

It is more convenient for our purposes to express the equation in the reduced form

$$\left(\pi + \frac{3}{\omega^2}\right) (3\omega - 1) = 8\tau$$

(the derivation of which can be found in most any thermodynamics text).

Figure 4 is a plot of the reduced van der Waals equation for several values of temperature. Note that each isotherm passes through or very close to its corresponding experimental point on the liquid saturation curve. But since the constants  $a$  and  $b$  are determined theoretically from conditions at the critical point, they cannot be expected to be exact for any but the critical isotherm. The region of primary interest is the liquid and superheated liquid condition for isotherms between  $25^{\circ}\text{K}$  and  $30^{\circ}\text{K}$ . In this area the curves agree very favorably with experimental data.

The equation of state, not being simple for the phase near or below the critical temperature, can best be represented by a power series expansion. Onnes (6) suggested such an expansion of the form

$$PV = A \left(1 + B/V + C/V^2 + D/V^3\right),$$

where  $A$ ,  $B$ ,  $C$ , and  $D$  depend only on the temperature and mass and are known as virial coefficients. Their values may be taken from experimental isotherms; in most instances the first and second coefficients are sufficient to define the curve.

To compare a plot of this equation with the van der Waals equation, it was first necessary to determine the values of the virial coefficients for the desired temperature. This was done by plotting the available data and using values taken from the curves (see Fig. 5).

A comparison was made of the isotherms for  $27.45^{\circ}\text{K}$ , since this is the midpoint in the region of primary interest. The comparison plot is shown in Fig. 6, and it can be seen that the shapes of the two curves

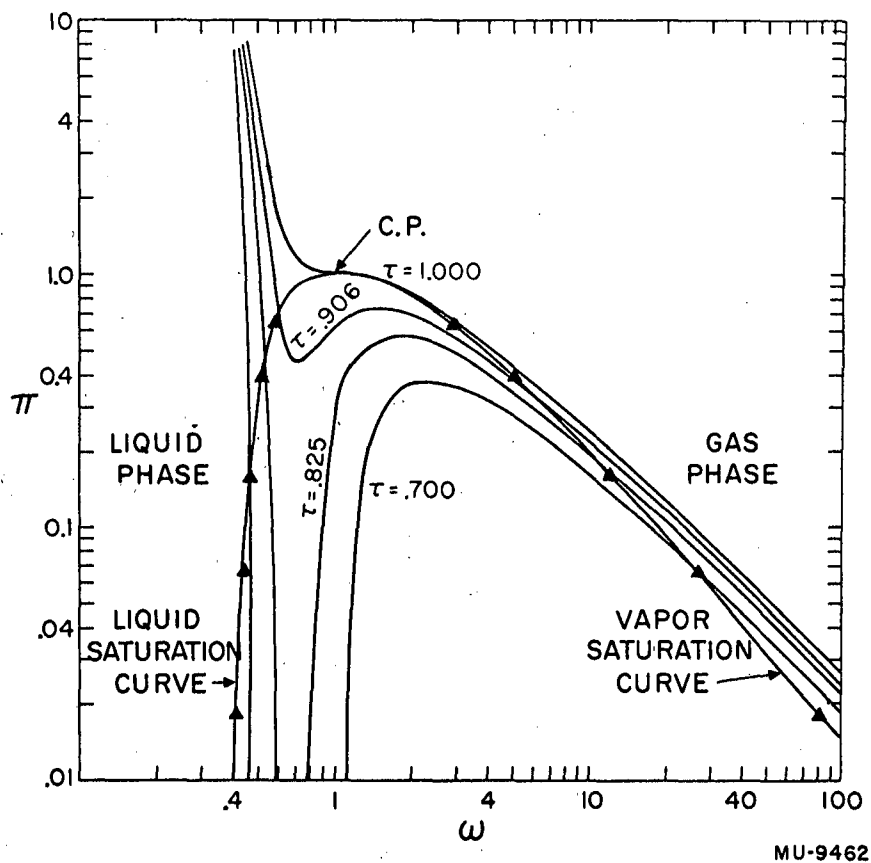


Fig. 4. Pressure-volume plots of the reduced van der Waals equation,  $(\pi + 3/\omega^2)(3\omega - 1) = 8\tau$ , for four temperatures. The liquid saturation curve is plotted from experimental data. Note that each isotherm passes through or very close to its corresponding experimental point on the liquid saturation curve.

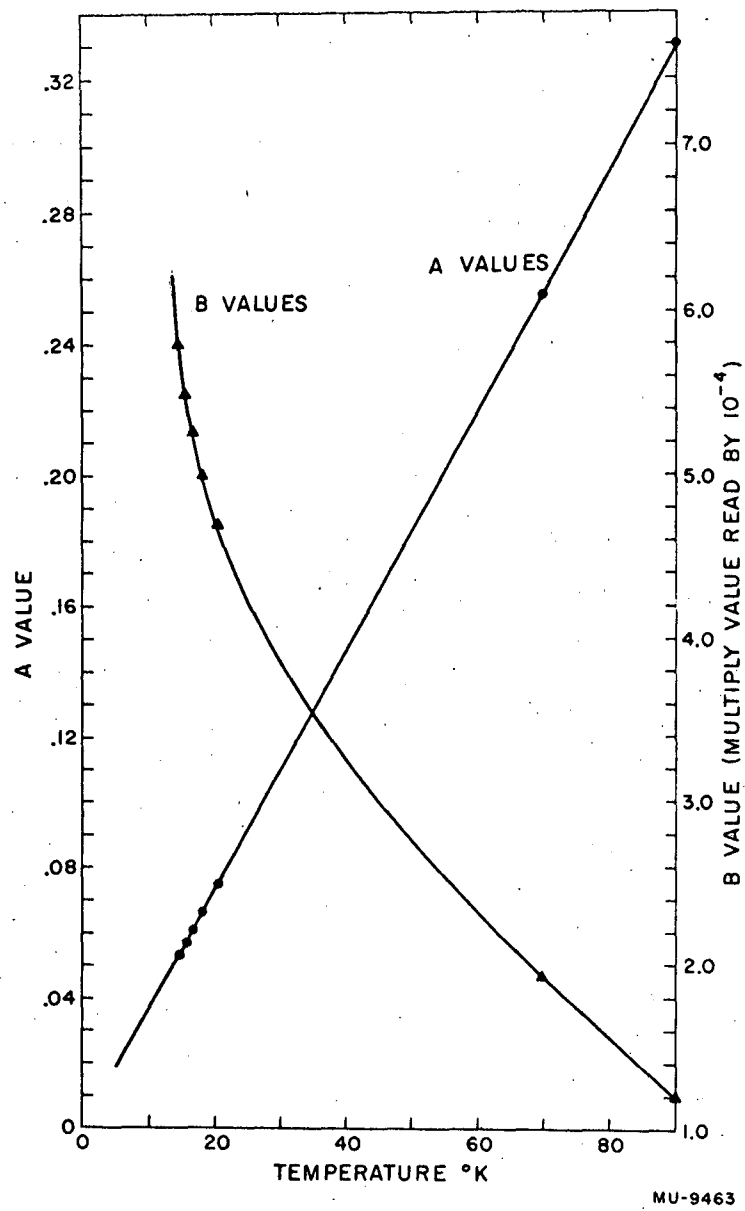


Fig. 5. A plot of the virial coefficients for hydrogen.

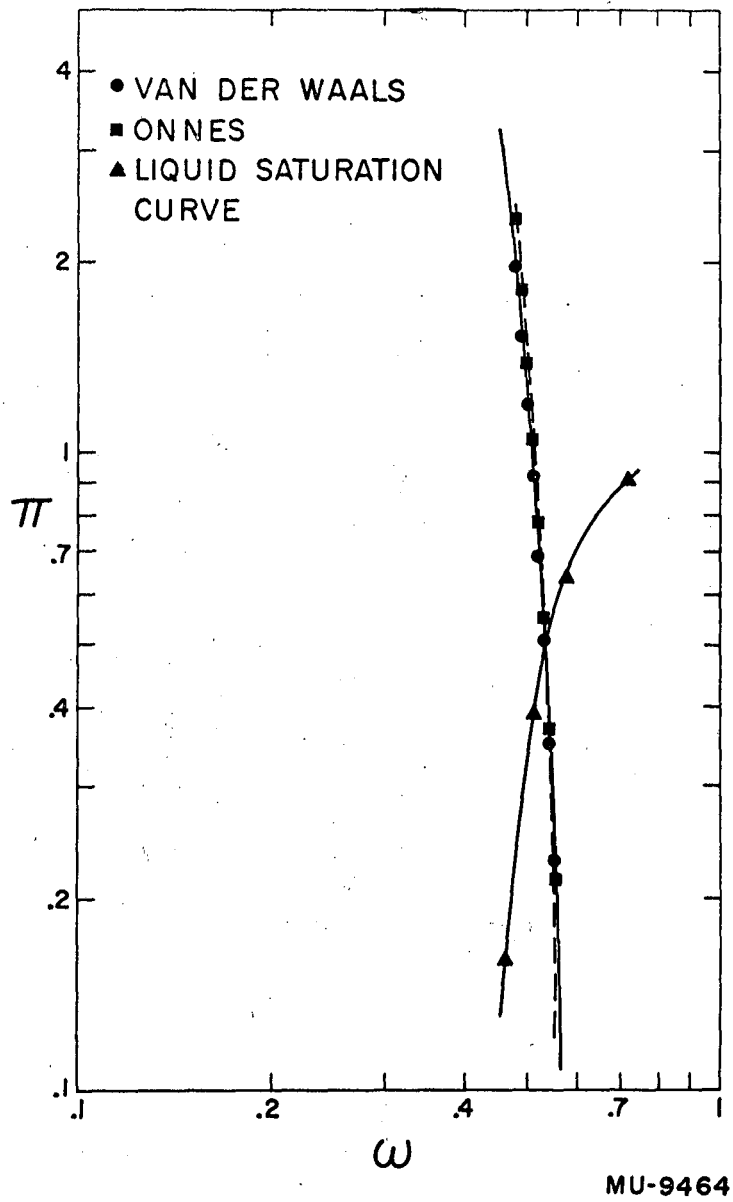


Fig. 6. A comparison plot of the van der Waals equation and the Onnes equation for hydrogen at 27.45° K. The liquid saturation curve is from experimental data.

are almost identical. Either curve should give excellent qualitative information.

### 3. Qualitative Analysis of the Thermodynamic Cycle.

Having ascertained that we have a reliable thermodynamic curve to work from, we may next consider a qualitative analysis of the thermodynamic cycle taking place in the bubble chamber. To be perfectly general, we could first identify each process as polytropic, where

$$PV^n = \text{Constant},$$

find the end points of pressure and volume, and determine the value of the exponent from the relation

$$n = \frac{\log (P_2/P_1)}{\log (V_1/V_2)}$$

From a practical standpoint, however, the design of the four-inch chamber is not ideally suited to such a procedure. Estimates would have to be made of the values of pressure and volume at each point. The difficulty in measurement of volume arises because at no time do we know what portions of the pipeline used to fill the chamber contain only liquid or vapor. Pressure measurements could be made, but they would not be reliable since a pressure gradient does exist throughout the volume. It would be far better, it seems, to examine the data obtained while operating the chamber and see if they can be made to fit familiar thermodynamic equations for frictionless non-flow processes. It so happens that this is entirely possible if minor assumptions are permitted.

Consider first the expansion cycle. This can best be described as an adiabatic process. It is well within reason to assume that owing to the almost instantaneous expansion no heat will flow into or out of

the liquid. We should expect some cooling to result from the rapid expansion of the liquid-gas mixture through the filling-expansion line into the expansion chamber. This in fact does happen, and is recorded by the temperature-measuring thermocouples.

Next let us consider the period immediately after the expansion and preceding the compression. This is when the boiling occurs and the total volume (liquid plus vapor) is fixed. Therefore, the only logical idealization is that of a constant-volume process.

The compression cycle is much slower than either of those preceding it; therefore we can expect a more complicated process. Referring to Fig. 3 again, we see that we are now at a point where liquid and gas coexist in stable equilibrium. Throughout the cycle the temperature of the chamber increases, reaching its original value when the compression is completed. Let us assume that the first part of the cycle is one of almost constant pressure until we reach the liquid saturation curve. From this point to our original point we must conclude that the process is one for which

$$k > n > 1,$$

where  $k$  is the "n" value for an adiabatic process ( $PV^n = \text{constant}$ ) and  $n = 1$  for an isothermal process.

This, of course, is a very approximate qualitative explanation of what is happening thermodynamically to the liquid in the bubble chamber. An analysis of the cycle, taking into account all the various factors such as variable specific heat, time elements, and the effect of heat flow to and from the regenerator in the filling-expansion line, is not possible at this stage of development of the four-inch chamber.

## CHAPTER III

### BUBBLE FORMATION AND GROWTH

#### 1. Nucleation.

In the previous chapter it has been shown that under the proper conditions a liquid can become superheated, and that this superheated liquid boils immediately if disturbed. It is this property of liquids which provides the foundation of bubble chamber operation.

The exact mechanism by which bubble nuclei are formed in the chamber is still somewhat in doubt. Two main theories have been proposed attributing this phenomenon either to local heating along the track of the particle or to small concentrations of ions of the same sign along the track. For the purpose of this paper it is sufficient to assume that, owing to an increase in the local energy density along the track of an ionizing particle, a series of bubble nuclei is formed.

#### 2. Bubble Growth.

The forces acting on an uncharged bubble are the pressure  $P_{\sigma}$  due to surface tension and the external pressure  $P$  of the liquid, both tending to collapse the bubble, and the vapor pressure  $P_{vp}$  within the bubble, tending to make it grow. It is easy to show that

$$P_{\sigma} = 2\sigma/r,$$

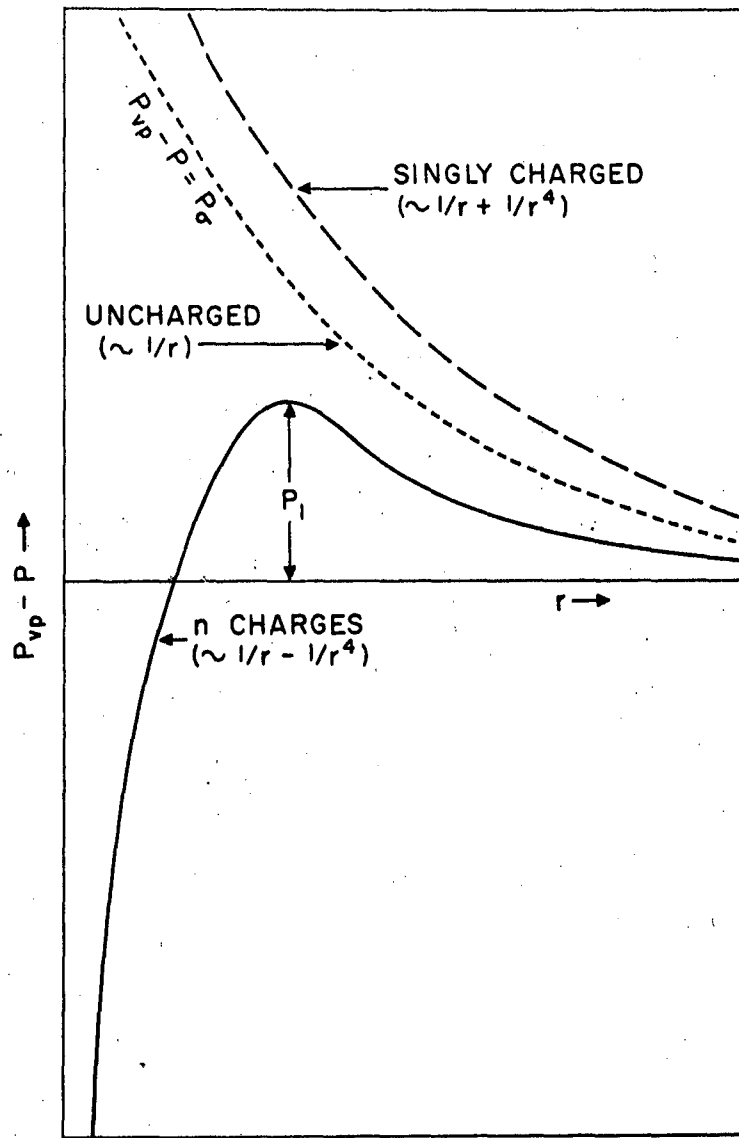
where  $\sigma$  is the surface tension constant and  $r$  the radius of the bubble. Thus, for very small bubbles, the surface tension seriously retards further growth. As the radius increases, the effect of the surface tension becomes progressively less, and the cooling effect of the heat transfer from liquid to vapor, with an attendant decrease in  $P_{vp}$ , becomes the limiting factor in the rate of growth.

Let us consider the growth of the bubble as divided into two phases.

There is no sharp line of demarcation between them, but we can define them broadly as follows: The first or initial phase is that period during which the surface tension is the significant factor, and the second phase is that interval wherein the surface tension is of minor importance and the cooling effect predominates.

If we now assume a bubble of such radius that the pressure due to surface tension is equal to the difference between the vapor pressure within the bubble and the external pressure, we have a condition of unstable equilibrium. Any change in vapor pressure or external pressure will cause the bubble to collapse or to grow. This condition of equilibrium is shown by the dotted curve of Fig. 7. A bubble located to the left of this line would collapse, since  $P_{vp} < P + P_{\sigma}$ . One to the right of it would grow. Therefore any bubble nucleus as described thus far would tend to collapse immediately if no additional force were brought into play. Its very existence is dependent upon some other factor arising to assist it during this initial phase of its growth.

Glaser (7) has formulated an approximate theory of the stability of charged bubbles in a superheated liquid, wherein he attributes this growth-aid contribution to charges trapped within the bubble. If a single charge is inserted in the bubble, it can be shown that this charge will run to the surface of the bubble. Glaser assumes that this charge is trapped at the bubble wall, and that the local binding energy is independent of the curvature of the surface of the wall. Using macroscopic continuum electrostatics, he calculates the rest of the energy and determines a new equilibrium condition. The energy contribution of its electric field will be negative and will tend to collapse the bubble. The equivalent electrostatic pressure  $P_{es}$  will be inversely proportional to the fourth power of the radius. The resulting new



MU-9465

Fig. 7. Equilibrium curves for bubbles of small radius.

equilibrium condition is shown as the dashed curve on Fig. 7.

If a number  $n$  of charges is trapped within the bubble, they will distribute themselves fairly evenly over the surface. Assuming these charges to be "smeared" smoothly over the bubble's surface, one again finds the equivalent electrostatic pressure inversely proportional to the fourth power of the radius, but now the energy contribution of the charges is positive and will assist the growth of the bubble. This last equilibrium condition is shown by the solid curve on Fig. 7; at any point above the curve,  $P_{vp}$  is greater than the sum of the other sources of pressure. Under these conditions, it is necessary to have only sufficient superheat to cause  $P_{vp} - P$  to exceed the pressure  $P_1$  shown on the figure in order for the bubbles to grow.

If there are only two or three charges in the bubble, the result is somewhat doubtful. It depends on the precise shape of the bubble and the means by which the charges are prevented from escaping from the bubble. As the number  $n$  increases, however, assumptions made in the development of the theory become more valid, and the results more nearly correct. The exact shape of the equilibrium curve depends on  $n$ . As  $n$  increases,  $P_1$  decreases. Thus by proper choice of the amount of superheat obtained, one can suppress bubbles containing less than a certain number of charges.

We now get into the second phase of growth. It is this phase in which we are most interested, as it is in this phase that the bubbles grow to visible size. In 1917 Lord Rayleigh (8) shed some light on the phenomenon of bubbles. He considered the question of the collapse of bubbles as a problem in the hydrodynamics of an incompressible fluid. Rayleigh's equation was

$$\rho \left( r \ddot{r} + \frac{3}{2} \dot{r}^2 \right) = \Delta P .$$

where  $\rho$  is the density of the liquid,  $r$  the radius of the bubble, and  $\Delta P$  the difference between the pressure inside the bubble and that at considerable distance outside the bubble. Rayleigh assumed  $\Delta P$  to be constant and neglected the heat transfer from liquid to vapor. This equation also neglects the retarding effect of surface tension. His end result was a growth rate almost linear with time.

Recent papers have explored in considerable detail the modifications to Rayleigh's theory encountered when corrections are applied to the equation to account for the factors previously ignored. Plesset and Zwick (9) approached this question by extending the Rayleigh equation to account for the surface tension effect,

$$\rho(r \ddot{r} + \frac{3}{2} \dot{r}^2) = \Delta P - 2\sigma/r,$$

and by modifying it further to account for the cooling effect of evaporation. They assumed viscous effects and pressure and temperature gradients in the bubble to be negligible, and neglected the effects of compressibility and buoyant forces. They further assumed the vapor pressure in the bubble to be approximately equal to the equilibrium vapor pressure of the liquid. The heat that is transferred to the bubble per unit time is

$$\dot{Q} = \frac{4\pi}{3} L \frac{d}{dt} (r^3 \rho'),$$

where  $\rho'$  is the vapor density and  $L$  the latent heat of evaporation per unit mass. As this heat must be furnished by the liquid, the heat loss in the liquid must be

$$\dot{Q} = 4\pi r^2 k \left( \frac{\partial T}{\partial r} \right)_R,$$

where  $k$  is the thermal conductivity of the liquid and  $\left( \frac{\partial T}{\partial r} \right)_R$  the temperature gradient in the liquid at the boundary. They finally derive a new equation of motion. From this, two solutions are obtained, one for bubbles of very small radius and one, which they

call the "asymptotic" solution, covering the later period where the heat diffusion from the liquid to the vapor is the limiting factor in the increase of the radius. Matching these two solutions by shifting the asymptotic solution in time, they obtain an expression that predicts for the radius a growth rate approximately proportional to the square root of time in the region where terms on the order of  $t^{-1/2}$  become negligible and where the bubbles grow to visible size.

Forster and Zuber (10) have also developed a theory based on the extended Rayleigh equation. Their approach was to relate the pressure difference  $\Delta P$  to the temperature difference  $\Delta T$  by the Clausius-Clapeyron equation

$$\Delta P = \frac{L}{T(v_1 - v_2)} \Delta T,$$

where  $L$  is the latent heat of evaporation,  $T$  is the temperature and  $v_1$  and  $v_2$  are the specific volumes of the vapor and liquid respectively. They obtained  $\Delta T$  from a solution of the heat conduction problem and, ultimately, also arrived at a growth rate approximately proportional to the square root of time in the region where bubbles are visible.

### 3. Experimental Results.

Operating-time assignments have thus far been at a premium for the four-inch bubble chamber. No opportunity has been available to make the ideal experimental setup for bubble-growth measurements. Such a setup must include a high-speed motion picture camera and a light source of comparatively long duration. The duration of the illumination of the present stroboscopic lamps is on the order of a few microseconds. A duration more on the order of 100 milliseconds would be required for good bubble-growth measurements.

Preliminary studies of bubble growth have been made by the authors. The data obtained thus far have been too meager and the

possible errors too great to permit drawing accurate conclusions, but the results are fairly consistent with theoretical predictions. Figure 8 is a logarithmic plot of bubble-growth measurements taken on three separate occasions. The data were obtained by measuring the sizes of a number of bubbles on photographs taken at specified times after passage of the ionizing particles. A curve,  $r = 0.06\sqrt{t}$  (where  $r$  is in millimeters and  $t$  is in milliseconds), is drawn to indicate the trend of the plotted points (no attempt was made to fit curves to the experimental data). Several sources of error may be associated with each point; namely, temperature fluctuations, uncertainties in the time delay between the passage of the beam and the taking of the photograph, the variation found in the sizes of bubbles in any one photograph, and the difficulty of accurately measuring any individual bubble. The temperature of the liquid hydrogen was  $27.5^{\circ} \text{K} \pm 2.5^{\circ} \text{K}$ . The instrumentation for measuring the time delays could have permitted errors of  $\pm 20$  percent in the timing. Some typical errors associated with the variation in bubble size are indicated on the plot. Inaccuracies in the measurement of individual bubbles are considered negligible by comparison.

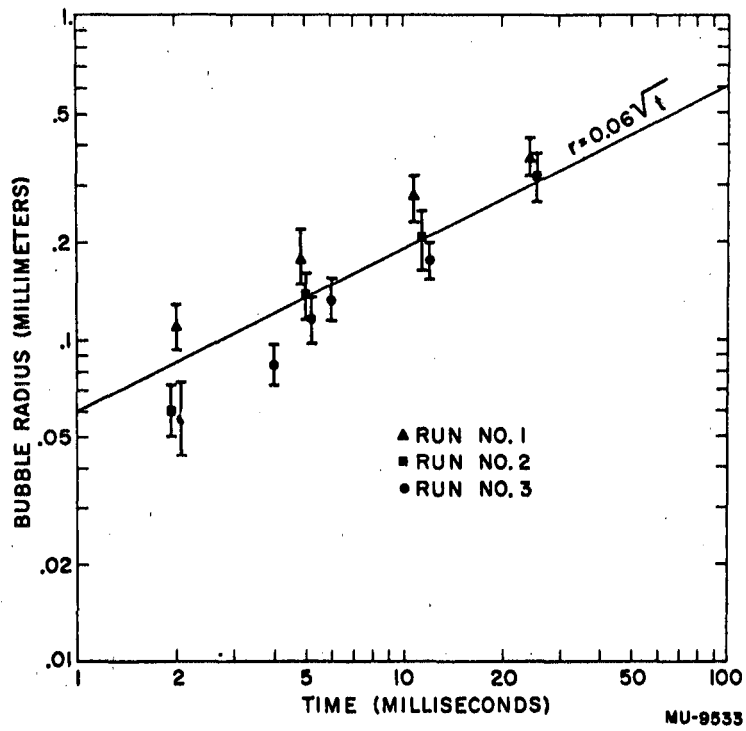


Fig. 8. Plot of bubble-growth data from preliminary study. The curve,  $r = 0.06\sqrt{t}$ , shows the trend of the plotted points and is not fitted to the data.

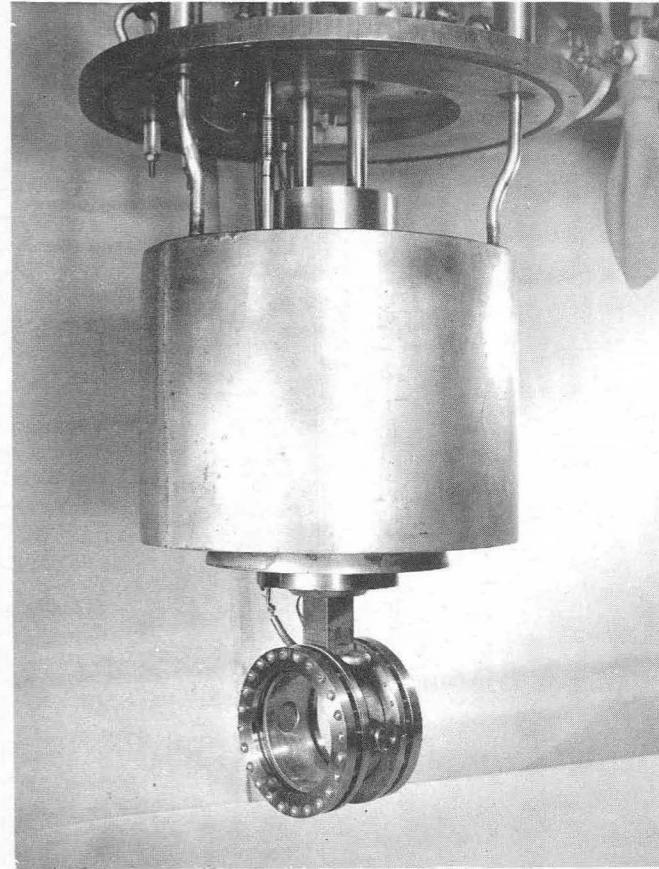
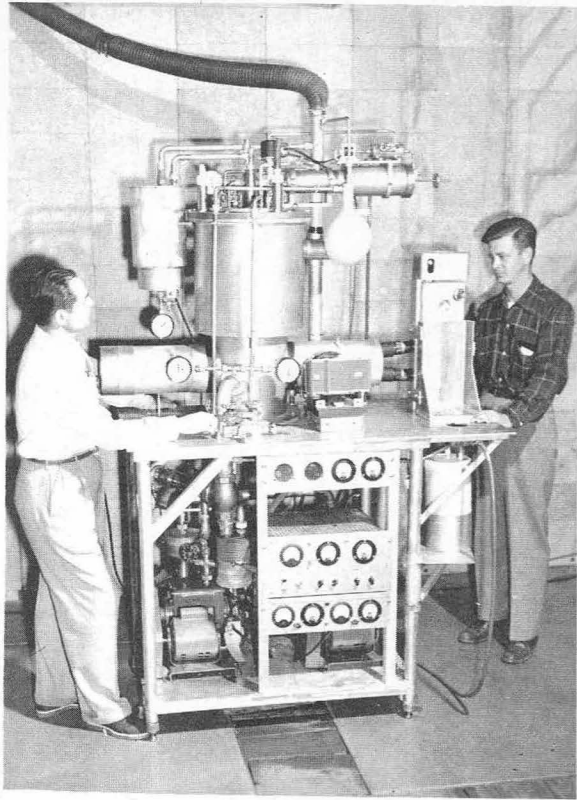
## CHAPTER IV

### CONSTRUCTION AND OPERATION

#### 1. Construction Features.

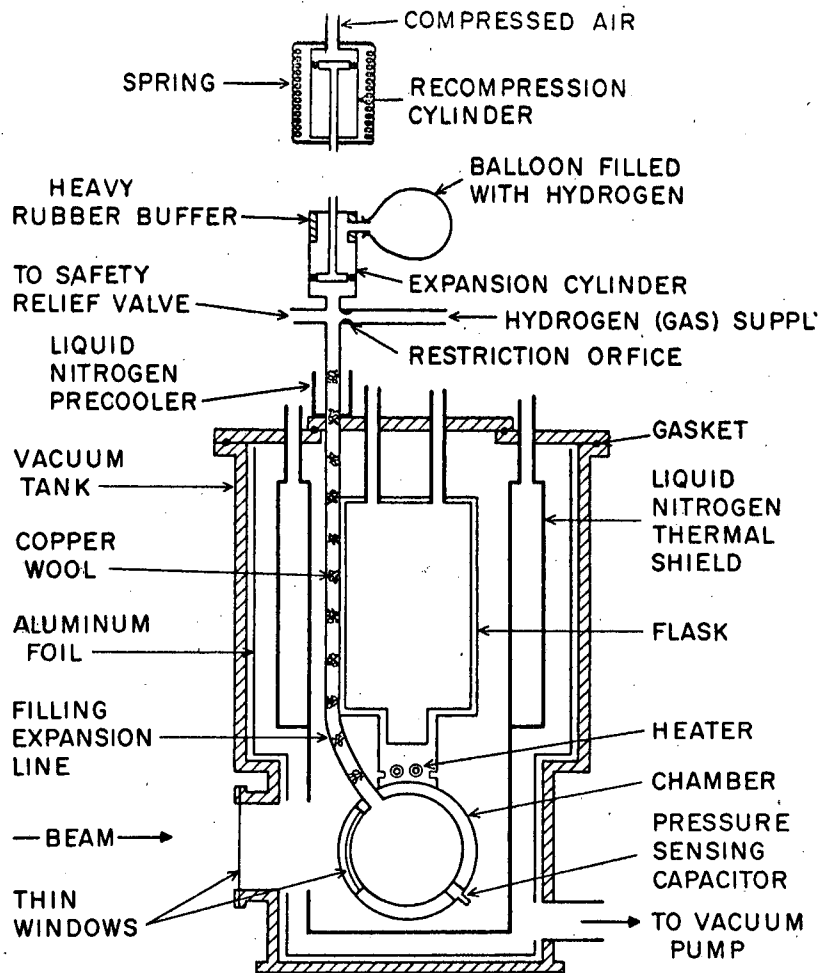
Figure 9 shows two views of the four-inch liquid hydrogen bubble chamber with the modified expansion system as described in Chapter VII. Figure 10 is a schematic diagram of the construction of the four-inch chamber system. The outside tank is a brass cylinder of 0.25-inch wall thickness which serves as a mount for the other components and as the vacuum tank for the entire system. In the walls of the bottom section of the tank are cut three large ports. Two are covered with pyrex glass for viewing and photography. The other is covered with a thin metal window, and is the point for entry of the beam. All ports are held on with a metal ring bolted to a flanged section and use soft rubber gaskets. The tank is lined with a layer of aluminum foil which reduces the emissivity of the wall of the tank. The vacuum system is simply a Kinney pump coupled with an oil diffusion pump. This gives pressures of the order of  $10^{-6}$  mm of mercury.

Inserted from the top of the vacuum tank is a stainless steel doughnut-shaped tank with a stainless steel skirt. In the skirt are cut two viewing ports and a port where the beam passes through to the chamber. This tank has a capacity of about twenty liters and is filled with liquid nitrogen. It serves as an additional thermal shield and establishes a permanent heat gradient between the vacuum-tank wall and the chamber. To minimize the losses of nitrogen due to boiling, the tank is suspended from a washer-shaped top plate by three thin-walled 0.50-inch-diameter stainless steel tubes. These tubes offer a high resistance to leakage of heat and provide a means for filling and



ZN-1261

Fig. 9. (a) The complete liquid hydrogen bubble chamber assembly. (b) The liquid nitrogen thermal shield (with skirt removed), the flask, and the chamber.



MU-9466

Fig. 10. The construction details of the four-inch liquid hydrogen bubble chamber assembly: schematic diagram.

venting the tank.

The final unit to be placed into the vacuum tank consists of the flask and the chamber. The flask is a cylinder of welded stainless steel construction, which is filled with liquid hydrogen. It is the cooling reservoir for the chamber. In operation it is maintained at atmospheric pressure, corresponding to a constant temperature of  $20^{\circ}$  K. It has a capacity of about six liters. The most ideal situation would be to isolate the flask from the outside, thereby reducing to a minimum the losses and fluctuation due to ambient thermal influences. This ideal situation is obviously impossible to attain; however, an acceptable solution is to duplicate the method employed in suspending the nitrogen tank. The flask is attached to a top plate by two thin-walled stainless steel tubes of 0.75-inch outside diameter. These tubes provide a means for filling and venting the jacket, and isolate the flask thermally.

Soldered over a hole cut into the bottom of the flask is a copper bar, hollowed out for about one half its length, and containing a resistance heating element. This bar is the controlled heat leak between the chamber and the flask. In operation, a fine control of the temperature of the liquid hydrogen in the chamber can be obtained by adjusting the pressure maintained on the chamber and by the use of the heating element.

The chamber is made of brass and is soldered to the copper bar. It is a cylinder of four inches inside diameter and two inches depth. The walls are 0.75 inch thick except for the region where the beam is to enter. Here the wall thickness is reduced to 0.125 inch. The ends of the cylinder have a flanged section into which is cut a V-shaped groove 0.030 inch deep to position a lead gasket. The ends are covered

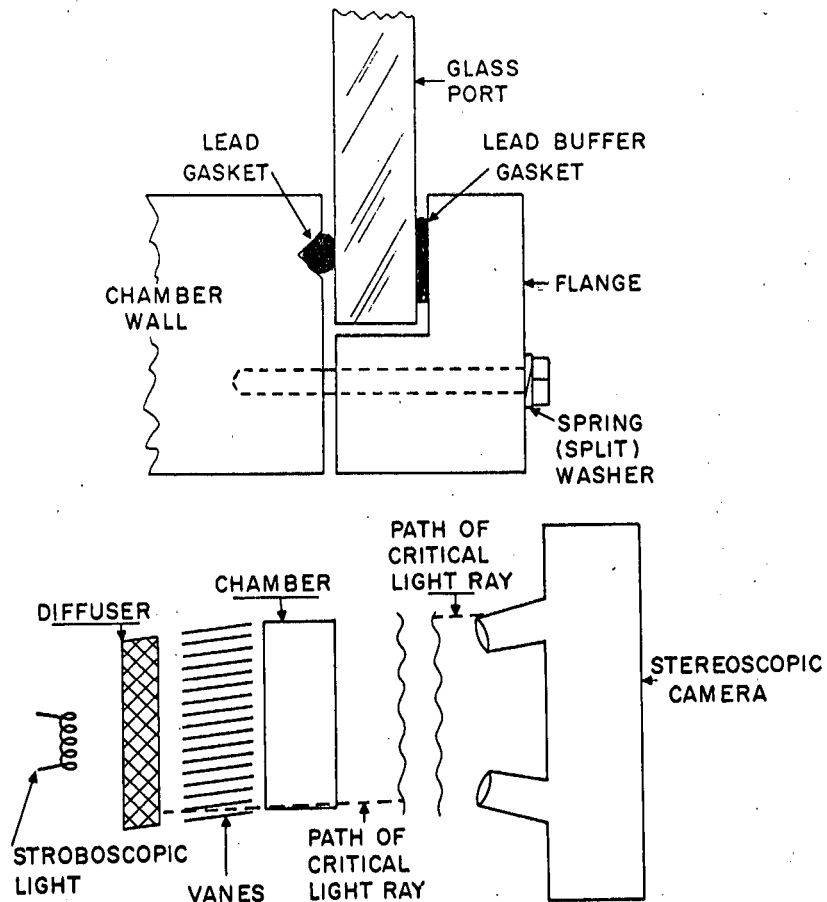
by 0.50-inch-thick pyrex glass optically polished and tempered. Finally brass rings are bolted to the flange to hold the glass in place.

The particular difficulty in this detail of construction was in the establishment of an effective seal between the glass and the brass chamber. A search of the literature revealed no information that this had been attempted at temperatures approaching  $20^{\circ}$  K, there apparently being no desire by cryogenicists to obtain visual observations at extremely low temperatures. Of the several methods tried -- notably Kovar metal, indium, solder, teflon, and gold -- in each instance either the glass cracked or the gasket material had a coefficient of expansion such as to make an undependable seal. Common lead finally provided a satisfactory solution to the problem.

A strip of sheet lead is carefully cleaned to remove all traces of lead carbonate, and is drawn through dies to produce a wire about 0.050 inch in diameter. The wire is shaped into a ring of proper diameter; the ends are carefully squared off, and soldered.

To maintain even pressure on the gasket, the brass ring is fastened on with many closely spaced bolts which are spring-loaded with split lock washers. In addition, another flat lead buffer gasket is placed between the glass and the ring to help distribute the load evenly on the glass when the bolts are tightened. The details of this construction are shown schematically in Fig. 11a.

Filling of the chamber is done through a 0.50-inch-diameter stainless steel tube called the filling-expansion line which passes through the top plate. This tube is kept in thermal contact with the outer wall of the flask. Inside the filling tube are small wads of copper wool, about 1.5 inches apart, which act as a heat regenerator (11) to maintain a controlled thermal gradient from the chamber at



MU-9468.A

Fig. 11. (a) Details of the glass-to-metal seals: schematic diagram. (b) The photography and illumination arrangement: schematic diagram.

20° K to the expansion cylinder at room temperature. Where it passes through the top plate, the tube goes through a larger open-ended cylinder (Precooler), which is filled with liquid nitrogen during the filling process, to precool the gaseous hydrogen. At the top the tube is attached to the filling and expansion system and a safety relief valve.

The filling system consists simply of a copper line extending first through a glass wool and charcoal trap immersed in a liquid nitrogen bath, then through a De-oxo unit to a pressure-regulating valve, and finally to a bottle of hydrogen gas. At the point where this line joins the filling-expansion line, a restriction orifice of 0.030-inch diameter is provided. This restriction serves to partially isolate the chamber and expansion system from the pressure in the filling line during the expansion cycle.

The expansion and recompression system consists of two cylinders containing free-travel pistons. These are at room temperature. One end of the expansion cylinder is connected to the filling-expansion line. The piston rod passes through an airtight packing box in a screw cap closing the other end. The piston is held in the extreme down position by a lever that engages a notch in the piston rod. The upper portion of the cylinder is lined with a heavy rubber buffer, which stops the piston at the end of its upward stroke. To prevent accumulating explosive mixtures of air and hydrogen in any portion of the cylinder, an opening is provided connecting the top section of the cylinder to a heavy rubber balloon which is kept full of hydrogen gas. Therefore, any leakage which may take place past the piston will be of hydrogen into a space already filled with hydrogen.

Mounted colinear with the expansion cylinder is the recompression

cylinder. The top of the cylinder is connected to a compressed-air line through a double-acting solenoid valve of large capacity. The piston rod extends through a hole in the bottom of the cylinder. No packing is provided here, since it is desirable that this side of the piston be open to the atmosphere for free operation. Attached to the end of the piston rod is a yoke, to the ends of which are connected springs that extend to the top of the cylinder where a similar yoke is fitted. These springs return the piston after the recompression stroke.

Photography is done with a stereoscopic camera. This is shown schematically in Fig. 11b. Vanes are placed between the light and chamber. They are slanted at such an angle that no direct light ray can reach the camera lens. (The only light entering the camera lens is that which is reflected or refracted by the bubbles in the liquid. This is dark-field illumination.) They are coated with a layer of dull black soot to minimize their visibility. The camera shutter remains open and photographs are taken by flashing the light. The bubbles, being the only points for light reflection and refraction, appear on the negative as dark spots against a light background.

## 2. Preparations for Operation.

In the preparation of the bubble chamber for operation, particular consideration must be given to the physics of low temperatures. Changes will occur in the physical size of the individual components due to their different coefficients of expansion. This can result in some extremely high stresses. Too rapid cooling can cause fractures due to the thermal shock. Experience also dictates other procedures that must be followed if successful results are to be obtained consistently. These will be pointed out.

The glass in the ports must be clean and free of scratches or they will become nucleation centers for bubbles when the chamber is operated. The condition of the remainder of the chamber is not critical as far as imperfections are concerned. Even though bubbles may (and do) form along the walls of the chamber, and in particular at the point of contact between the glass and the metal walls, these bubbles do not grow sufficiently fast to cause any obstruction of the view or to cause any serious decrease of superheat.

The removal of alien gases and water vapor from the chamber and from the expansion and filling systems is important. These gases and water vapor would solidify upon cooling, causing constrictions in the piping, and would contaminate the liquid in the chamber. Also, a potentially explosive mixture could result if some of the extraneous gas were free oxygen. The gases and water vapor are removed by evacuating the chamber and the expansion and filling systems with a Kinney vacuum pump and flushing several times with helium gas.

When the contaminating gases and water vapor have been removed, and the vacuum jacket has been evacuated, precooling is commenced. The liquid nitrogen thermal shield is filled. (It is refilled from time to time as necessary to make up for losses by boil-off.) This is usually done at least twelve hours in advance. The flask and chamber will now slowly cool, minimizing the possibility of thermal shock when they in turn are precooled.

Precooling of the flask and chamber is usually done in two steps. First the flask is filled with liquid nitrogen, which is then allowed to boil off. It should be ensured at this point that all the nitrogen is in fact boiled off. If any should remain it would solidify when the liquid hydrogen is put into the flask, and because of its location in the lower

part of the flask it would act as a thermal insulator, preventing the chamber from becoming cold enough to be filled. After the nitrogen is completely boiled off, the second step is to permit liquid hydrogen to drip slowly into the flask. This slowly cools the flask and chamber further, reducing the possibility of leaks at the port gaskets due to sudden contractions of the metal. This second step has been omitted on occasion without producing any adverse effect.

Final cooling is accomplished by filling the flask with liquid hydrogen. Filling of the chamber may now be commenced. The liquid nitrogen precooler is filled, as well as the liquid nitrogen bath for the charcoal filter. The hydrogen gas pressure in the filling line is raised to about four atmospheres, and within minutes liquefaction of hydrogen can be observed in the chamber. The chamber will fill completely within about one hour.

When the chamber is full, the pressure is increased to about five atmospheres and the heater in the chamber heat leak is regulated to increase the chamber temperature to approximately  $29^{\circ}$  K. When these conditions prevail, the heater is adjusted to maintain this temperature and the chamber is ready for operation.

### 3. Operation.

In this section let us first discuss the mechanical operation of the chamber. The use of the various delay sequences can then be considered.

To initiate an expansion and recompression cycle, a solenoid is actuated by a 40-millisecond high-voltage direct-current pulse, tripping the lever that holds the expansion piston in the down position. The piston is forced to the extreme up position by the pressure in the

chamber. The constriction in the filling line prevents the higher pressure in the line from being maintained in the chamber, and as a result the chamber pressure drops to approximately one atmosphere in about four milliseconds. In the meantime, when the lever was tripped to release the expansion piston it contacted a microswitch. This resulted in the sending of a signal to the other solenoid valve, porting high pressure air to the top of the recompression piston. Just at the time the expansion piston has come to rest against the rubber buffer, the recompression piston starts its recompression stroke, returning the expansion piston to its down position and recompressing the hydrogen in the chamber. A spring attached to the lever causes it to engage the notch in the piston, releasing the microswitch, which in turn results in the interruption of the signal to the solenoid valve. The high-pressure air is cut off and the air on the top of the recompression piston is ported to the atmosphere. The piston returns to the up position through the force of the two springs previously described. The entire cycle may be repeated about once every three to five seconds.

#### 4. Adjustment of Operating Conditions.

The variables that may be adjusted during operation are the chamber pressure, chamber temperature, beam time, and light time. The effect of each is now considered, with recognition that each must be adjusted in relation to the others if optimum results are to be attained.

Chamber pressure is limited at its maximum point primarily by the consideration of the stresses on the chamber, which are manifested by leaks around the lead gaskets or rupture of the glass. The maximum working pressure has never been permitted to exceed six atmospheres. Actually, there is no point in having the working pressure any higher

than is necessary to keep the liquid from boiling when compressed, since pressure is not the primary limiting factor on the amount of superheat obtained. Likewise, the minimum working pressure has never been lower than four atmospheres, because lower pressures do not permit obtaining a sufficiently high temperature to give the degree of superheat necessary for satisfactory operation.

Chamber temperature is the real controlling factor in the production of satisfactory tracks (this has been covered in the preceding chapters). A temperature between  $26^{\circ}$  and  $30^{\circ}$  K was found to be the most satisfactory. Owing to this spread in operating range a useful control becomes possible -- that of biasing out the tracks of minimum-ionizing particles. This phenomenon is more fully explained in the chapter on bubble growth. Figure 20a and 20b are photographs illustrating this feature.

The optimum setting for entry of the radiating beam is at the time of lowest chamber pressure. This is adjusted by use of electronic timing circuits and is covered in the chapter on control and instrumentation. Experiments have shown that the limit of sensitive time of the liquid is about 50 milliseconds, after which the degree of superheat becomes too small for satisfactory track production. Also at about the same time the bubbles that have formed on the walls of the chamber have begun to rise, obstructing the view of any tracks that may be present.

The stroboscopic light for photography is flashed between two and five milliseconds after beam time. Earlier photography does not permit sufficient time for bubble growth, the bubble tracks being too fine for clear definition. Later timing is unsatisfactory in that the individual bubbles in the tracks have become so large as to obscure

the tracks behind them. Also, turbulence of the liquid caused by the rapid expansion begins to show its effect by unpredictable anomalies in the track curvature. When the light delay is adjusted to permit adequate bubble growth to give clear tracks, no turbulence effects are noted.

## CHAPTER V

### CONTROL AND INSTRUMENTATION

#### 1. General.

In order to ensure that proper conditions within the chamber are easily reproducible and that the most effective interpretation can be made of the photographs obtained, it is mandatory that certain control and instrumentation facilities be provided. One must have a means for the measurement of and positive control over the chamber temperature, the initial pressure, and the relative times of events during the cycle of operation, as well as a means of measuring the actual pressures in the chamber during expansion. For the sake of convenience, automatic recording of some of these items is desirable.

This chapter applies primarily to the use of the bubble chamber in the beam of the Bevatron. The system described is typical and one that has been used. Specific features of operation with other accelerators require modification of the timing circuit, but other components are essentially unaffected.

#### 2. Timing Circuit.

The "brains" of the bubble chamber lie in the timing circuit. One such circuit is shown in block diagram form, together with approximate pulse shapes, in Fig. 12. Here use is made of one of a series of pulses called marker pulses generated by the Bevatron control circuit at predetermined times during its cycle of operation. These pulses are controlled by the Bevatron magnet current, and each occurs at a specific time in the Bevatron's cycle of operation and corresponds to a particular value of particle energy. A marker pulse, occurring some milliseconds before the beam, is chosen to initiate the bubble

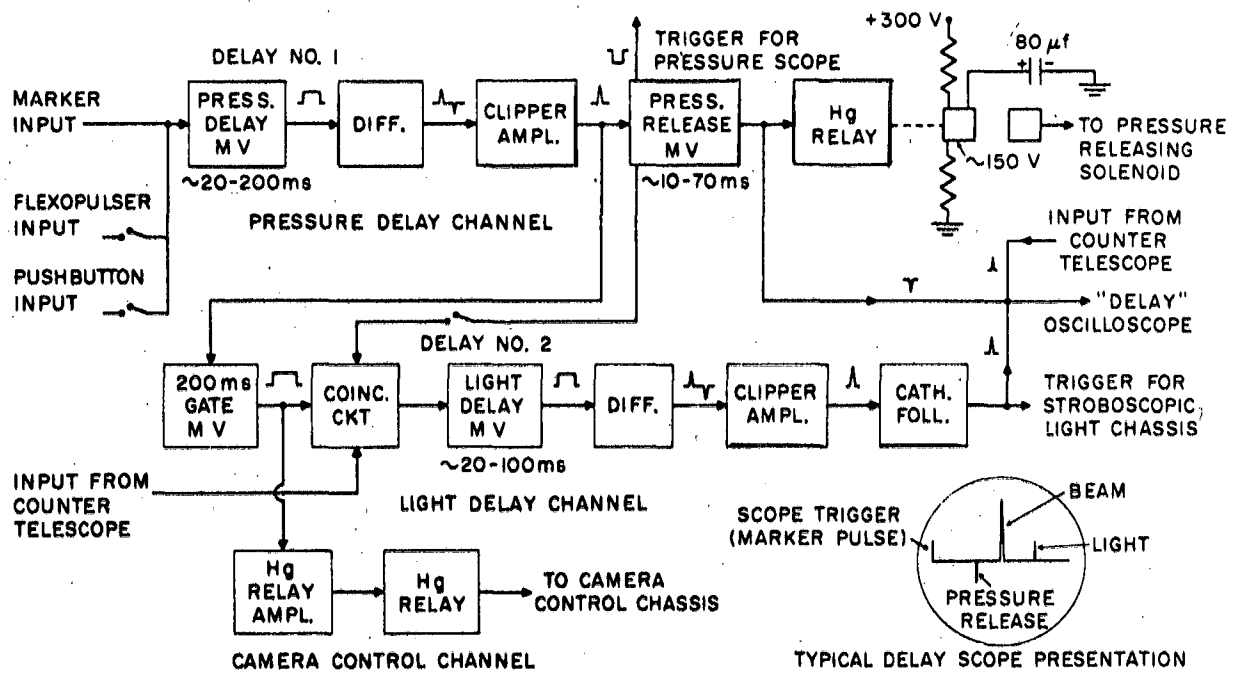


Fig. 12. Timing circuit for four-inch liquid hydrogen bubble chamber: block diagram.

MU-9469

chamber's cycle of operation.

This pulse is fed into a one-shot multivibrator in the pressure-delay channel. A positive output from the multivibrator is differentiated, and the tip of the second or negative pulse appearing in the output of the differentiator is inverted and amplified in the clipper amplifier. The amplified pulse is used to trigger a second one-shot multivibrator. The output of this multivibrator is used to close the contacts of a mercury relay permitting an 80  $\mu$ f condenser to discharge through the expansion solenoid, releasing the pressure in the chamber. From the above it is obvious that the release of pressure is delayed by an amount equal to the pulse length of the first multivibrator. This is variable between approximately 20 and 200 milliseconds. The actual delay chosen is of such duration as to place the beam timewise approximately at the minimum pressure point in the chamber operating cycle. The second multivibrator permits a pulse length up to about 70 milliseconds, and this is set at a value that will ensure almost complete discharge of the condenser before the relay contacts are opened. A signal from this multivibrator is also used to trigger the pressure-recording oscilloscope, discussed more fully in a later section.

The positive pulse from the clipper amplifier is also used to trigger a 200-millisecond gate circuit. This gate is fed into a coincidence circuit in the light-delay channel. At any time during this gate, an input from a counter telescope placed in the path of the beam will pass through the coincidence circuit and trigger the first multivibrator in the light-delay channel. This multivibrator output is differentiated and amplified in the same manner as in the pressure-delay channel. It is then fed through a cathode follower to flash the stroboscopic lamps used for photography. The delay in this channel is

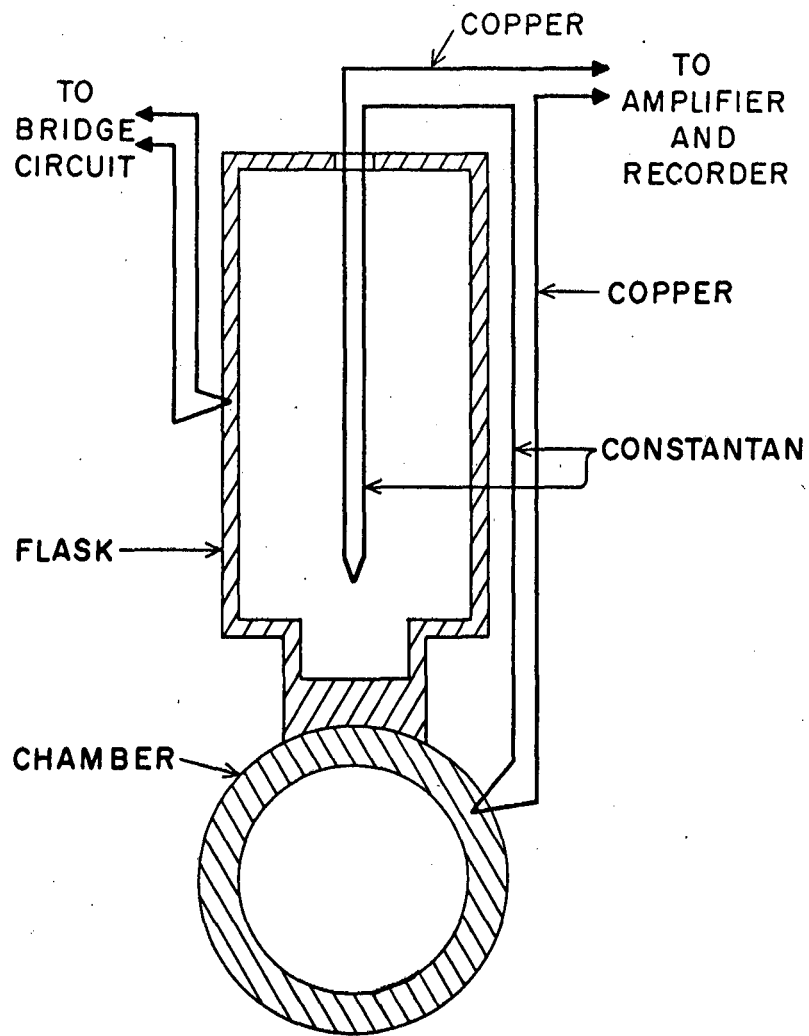
variable between approximately 20 and 100 milliseconds, and is used to photograph the track at that time after passage of the beam that will give optimum bubble size and resolution.

The output of the gate circuit is also amplified and used to close the contacts of a mercury relay and actuate the camera control mechanism.

In addition, outputs from the pressure multivibrator, the light trigger, and the counters are fed into an oscilloscope, triggered by the same marker pulse that starts the timing cycle, to give a complete picture of the timing sequence. A typical presentation of this oscilloscope is shown in Fig. 12. Both push-button and Flexopulser inputs are provided for test purposes; similarly, the pressure multivibrator output can be used in lieu of the counter output in the light-delay channel.

### 3. Chamber Temperature.

The chamber temperature is measured by means of two copper-constantan thermocouples connected back to back as shown in Fig. 13. This system makes use of the temperature dependence of the contact difference of potential generated at a copper-constantan junction. One junction is imbedded in the wall of the chamber, and the other suspended so that it hangs inside the flask several inches above the bottom. This latter junction, located in liquid hydrogen boiling at atmospheric pressure, is used as the reference. The two constantan leads are joined together. Then the voltage appearing between the two copper leads is the difference between the voltages generated at the two junctions and is thus a measure of the temperature difference between the flask and the chamber. This signal, on the order of 50 microvolts, is amplified to a few millivolts and displayed on a Leeds and Northrup



MU-9470

Fig. 13. Temperature-measuring arrangement for four-inch liquid hydrogen bubble chamber; schematic diagram.

Speedomax Recorder. Convenient tables are available to convert this voltage reading into temperature.

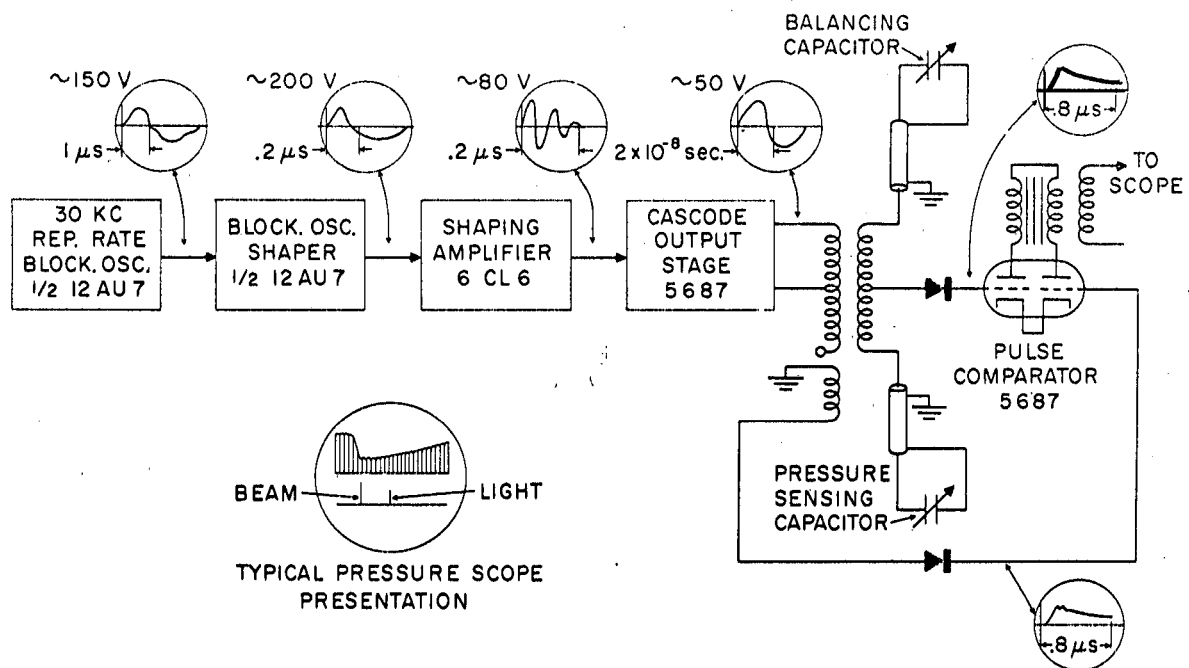
A third junction is shown imbedded in the side of the flask. The voltage generated here is fed directly into a bridge circuit and is used to give a rough indication of rapid changes in the temperature of the flask, occurring, for example, after all liquid nitrogen has been boiled out at the end of the precooling stage of operation. In this case the junction of the constantan lead with the copper terminal of the bridge at room temperature is used as the reference.

The temperature is controlled by varying the current through a resistance heater located in the copper block connecting the chamber to the flask.

#### 4. Pressure Measurement.

The pressure-measuring equipment, designed by William H. Linlor, is shown in block diagram form in Fig. 14. It uses a condenser microphone technique. A small parallel-plate condenser is mounted in the side of the chamber so that one plate of the condenser forms part of the chamber wall. The change in capacitance accompanying the deformation of this plate gives a measure of the pressure in the chamber.

A blocking oscillator generates a positive pulse of about one microsecond duration and with a repetition frequency of about 30 kc. The pulse length is decreased to about 0.2 microsecond in a second blocking oscillator, and is then fed into a shaping amplifier. The grid of the shaping amplifier is biased sufficiently negatively that the tube "sees" only the tip of the incoming pulse. This causes a "ringing" in a transformer in the plate circuit which is fed to the cascode output stage. The cascode stage sees only the first positive pulse of this



MU-9471

Fig. 14. Pressure-measuring circuit for four-inch liquid hydrogen bubble chamber; block diagram.

ringing, as thereafter a condenser in its grid circuit becomes charged sufficiently to bias out the remaining pulses. This results in a positive pulse about 50 volts high and  $2 \times 10^{-8}$  second long which is fed into one half of the primary of the output transformer. The other half of the primary is left dangling. Now, when the positive pulse is fed into one half of the primary, a negative pulse appears at the dangling end, and the net result is to minimize the effect of stray capacitance between the primary and secondary. The transformer secondaries are twisted together and wound in push-pull fashion. The pulses, identical except for sign, are fed into identical coaxial cables, one going to the pressure-sensing capacitor in the chamber wall and the other to a trimming capacitor. The trimming capacitor is to permit proper balancing of the two circuits in the static condition to insure that both are identical and give maximum sensitivity to changes produced by pressure variations in the chamber. The two coaxial lines act as open-ended transmission lines, modified only by the effect of the terminating condensers. Thus the pulses are reflected back, and the difference in the reflected signals is fed through a crystal diode into the grid of one triode of the pulse-comparator tube. Any change in the value of the pressure-sensing capacitor causes a change in this reflected signal. A reference signal is fed to the other grid of the comparator through a crystal diode by the small additional secondary of the transformer. The comparator then acts as a difference amplifier. The outputs of the two triodes appear on push-pull primary windings of a transformer in the plate circuit. The secondary of this transformer sees only the signal resulting from the pressure change in the chamber. This signal is displayed on an oscilloscope where it can be photographed for recording purposes. The crystal diodes and associated R-C

circuits serve to lengthen the pulses, thus easing the high-frequency requirements of the succeeding components.

The oscilloscope used here is a dual-beam type. The pressure variation is shown on the upper sweep, and the beam time and photograph time on the lower sweep. This affords a second means of verifying the relative times of events.

The initial pressure in the chamber is controlled by a pressure regulator in the gaseous hydrogen supply line. There is no means provided to vary the amount of pressure reduction when the chamber is expanded during normal operation. To vary this would involve removing the recompression cylinder and the top of the expansion cylinder and replacing the rubber buffer with one of a different size.

#### 5. Miscellaneous.

A camera control circuit is provided consisting primarily of a small electric motor controlled by a series of relays. This is used to reposition the film after each exposure. The operation can be started by the bubble chamber timing circuit, a Flexopulser, or a push button. When the film has reached the position for the next picture, a microswitch opens, turning off the motor. Another relay then opens, preventing the motor from being turned on again until the next cycle has begun. A simulated electronic camera has been built into the circuit to permit testing of the operation without wasting film. A series of pilot lights continuously shows the readiness state of the camera.

Also incorporated into the camera control is a counter for numbering the photographs serially. This is so mounted behind the camera that the register reading is recorded on the film between the two photographs of the stereoscopic pair. A second simultaneously

operated counter is mounted on an external control panel to facilitate proper correlation of observed data with the photograph.

To give an approximate idea of the intensity of the beam, the output from the counter telescope used to trigger the light -delay channel is also fed into a scaler-recorder on the external control racks.

## CHAPTER VI

### PHYSICS EXPERIMENTS

#### 1. Purpose.

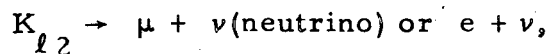
Preliminary experiments using the bubble chamber were designed primarily to prove its capabilities, potentialities, and general practicality as a detector. An analyzing magnetic field was not used because quantitative analysis of the tracks was not particularly desired at this stage of development. The chamber was operated at the 184-inch cyclotron and at the Bevatron; in each instance an exterior magnet was used to deflect a beam of elementary particles into the liquid hydrogen.

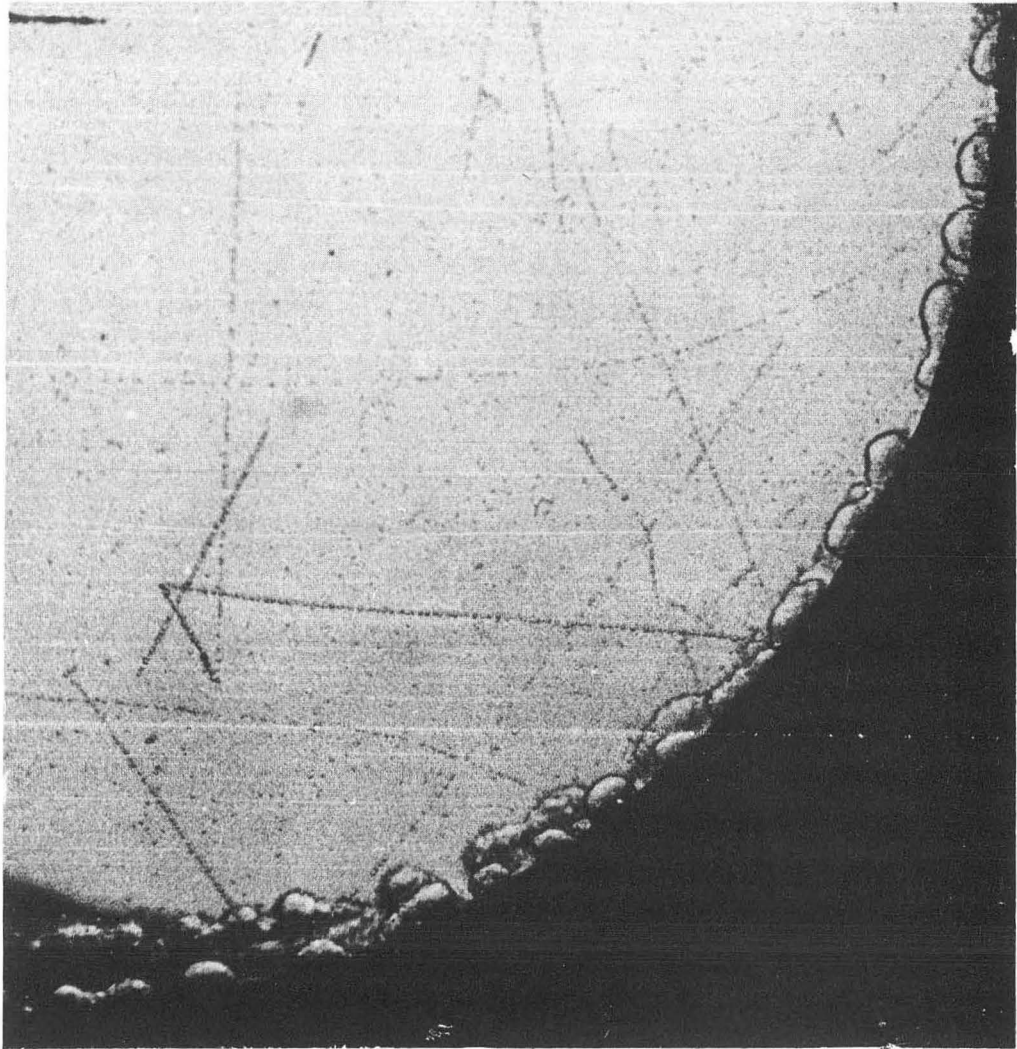
#### 2. The 184-inch Cyclotron Experiment.

The first run using the chamber at an accelerator was on November 19, 1954 at the 184-inch cyclotron. This was a low-energy  $\pi^+$  -  $p^+$  scattering experiment. Absorbers were placed exterior to the chamber. It was desired to see 10- to 15-Mev  $\pi$ -mesons stopped in the hydrogen. Among the more interesting events observed was a  $\pi$ - $\mu$ -electron decay. This is shown in Fig. 15.

#### 3. The Bevatron Experiments.

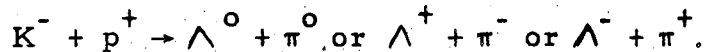
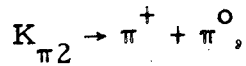
The succeeding runs were made with the chamber at the Bevatron. The first experiment was to investigate the interactions in hydrogen of high-energy  $\pi^-$ -mesons. Energies of the order of 3.5 Bev were used. The second experiment was a preliminary study of background contamination problems prior to beginning an investigation of the stopping of K-mesons in hydrogen. The K-meson has a rest mass of about  $960 m_e$ . Possible reactions to be examined are:





ZN-1190

Fig. 15. A  $\pi - \mu - e$  - electron decay in liquid hydrogen.



Some interesting events were observed during these experiments at the Bevatron. Figure 16 is identified as a possible  $\pi^-$ - $p^+$  elastic scattering. Figure 17 is a stereoscopic view of what appears to be the decay of a V-particle, the reaction being

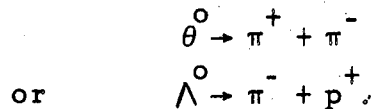
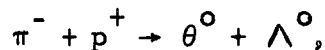
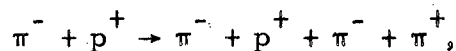


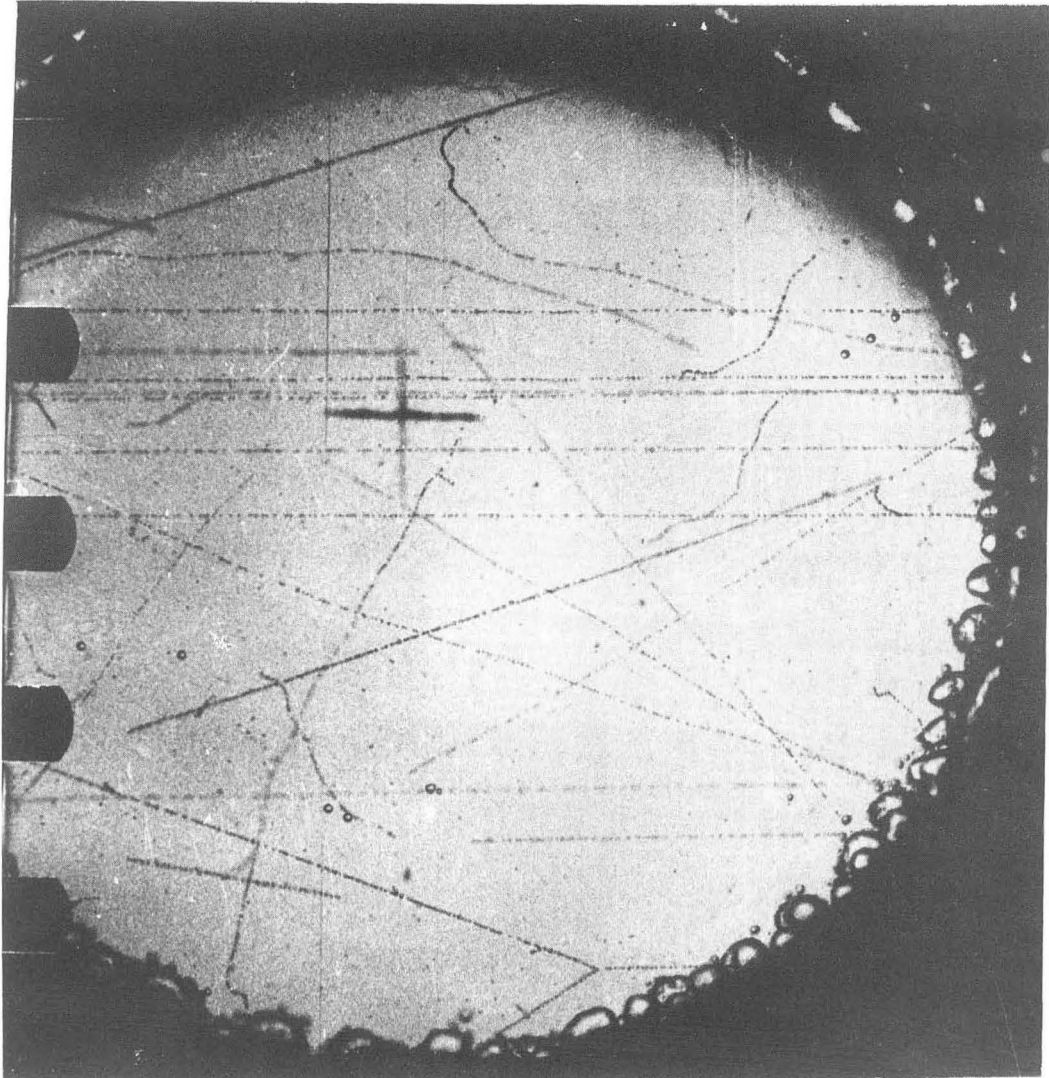
Figure 18 is an even more interesting event, that of a V-particle being created through the possible reaction,



one of the V-particles then decaying. Figure 19 is another stereoscopic view showing a  $\pi^-$  entering from the right and the creation of a four-pronged star. This has been identified as a possible reaction,

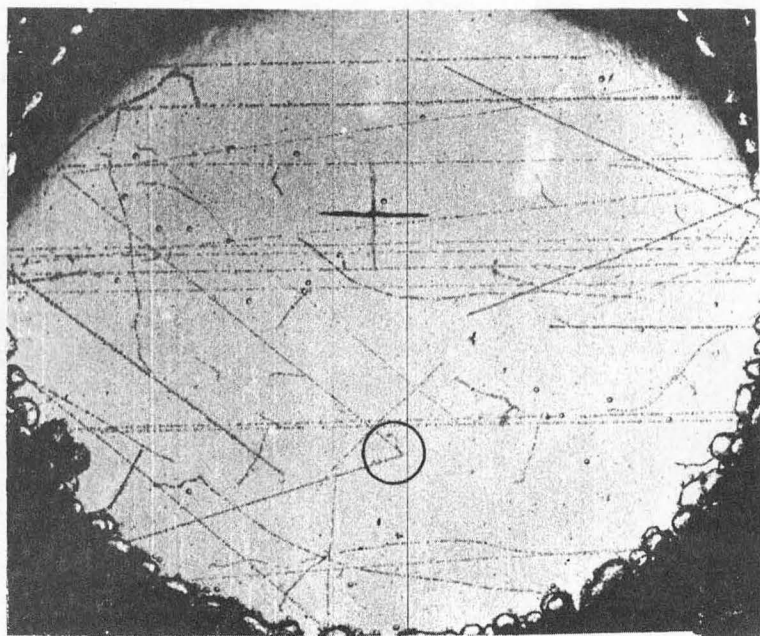
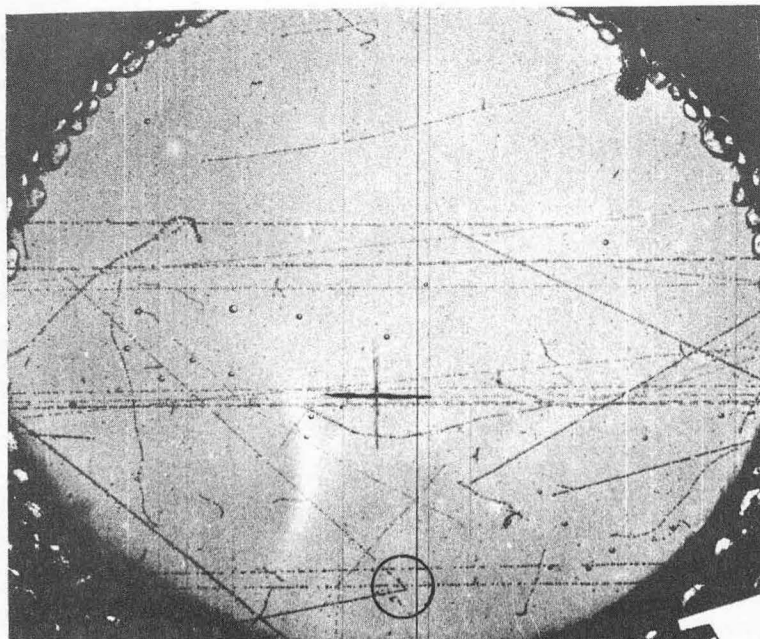


that is,  $\pi$ -meson pair production.



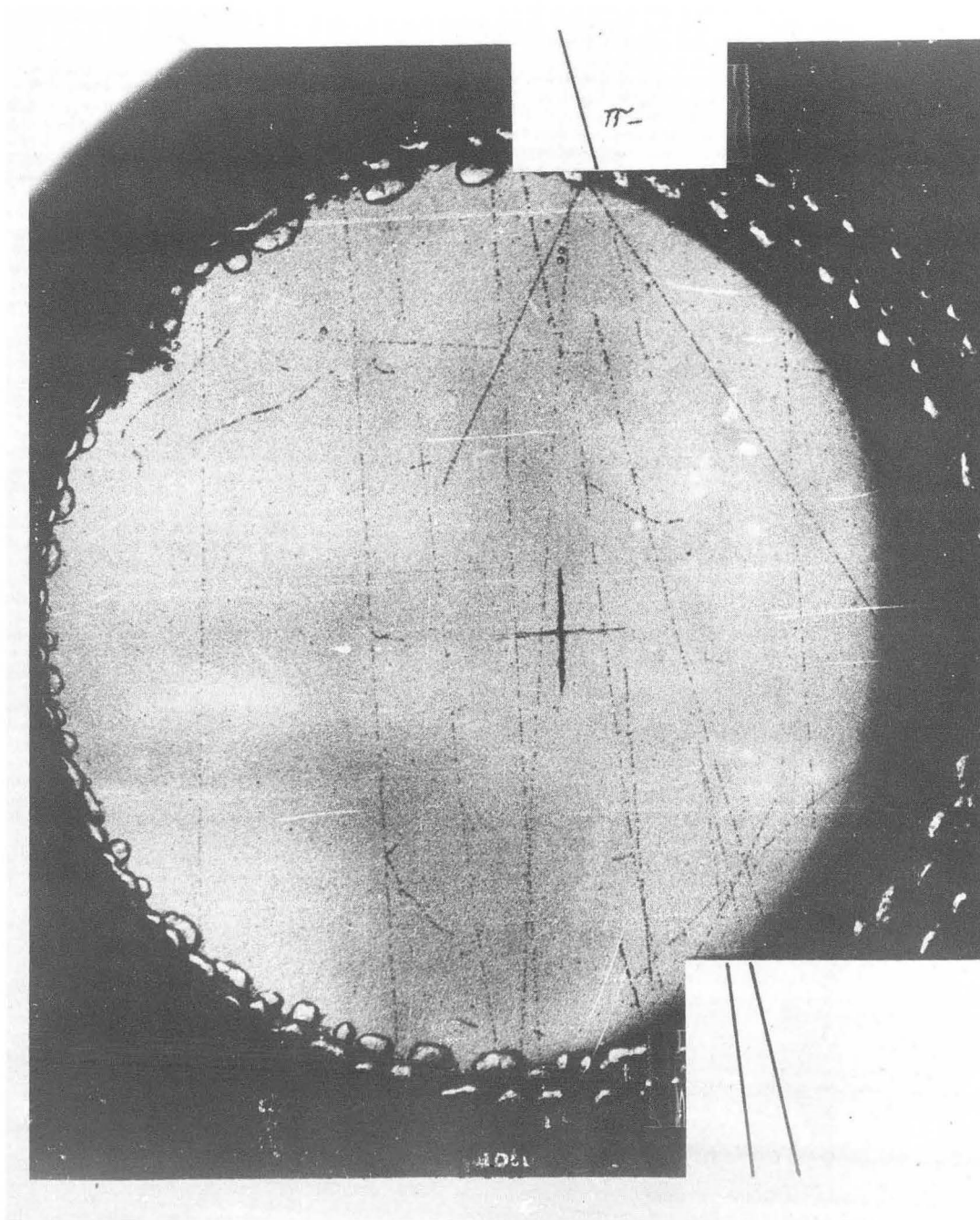
| ZN-1192

Fig. 16. A  $\pi^- - p^+$  elastic scattering event.



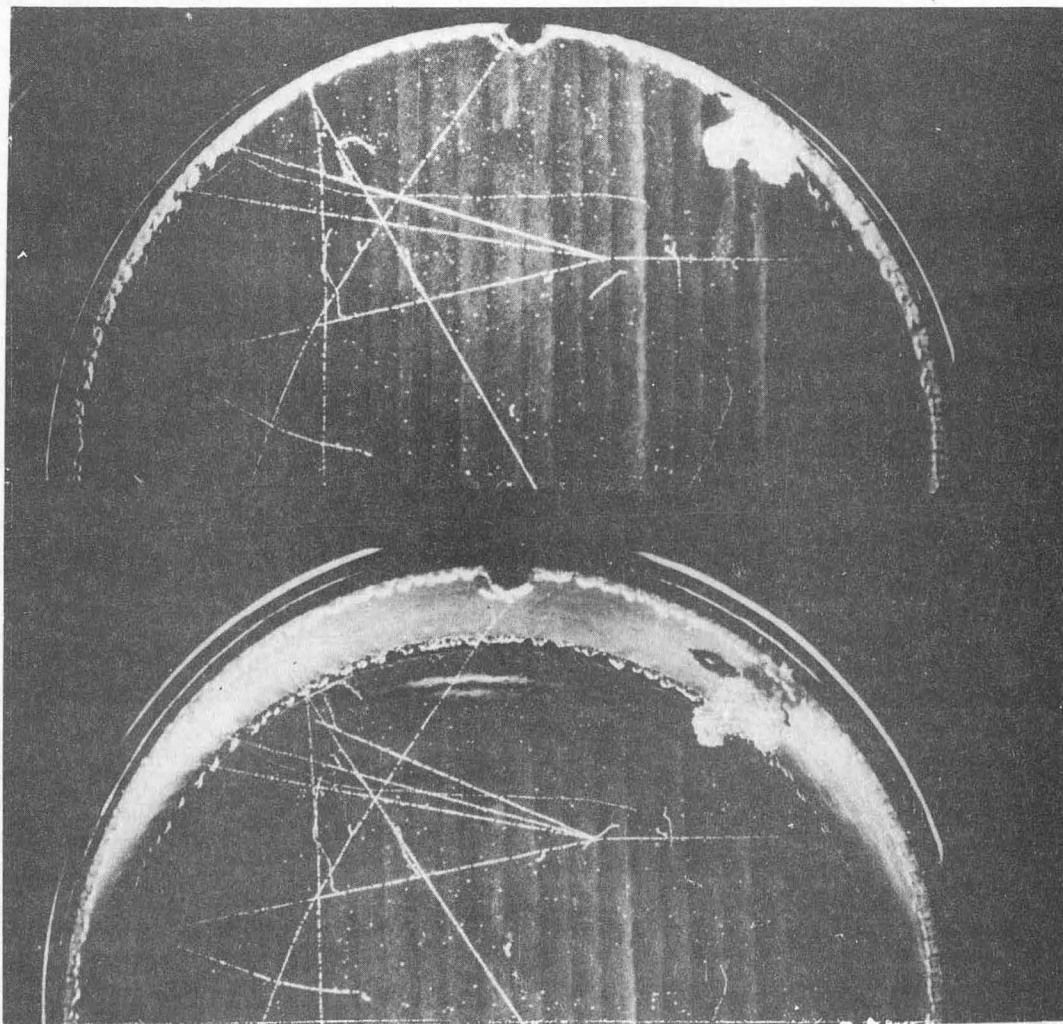
ZN-1193

Fig. 17. A stereoscopic view of the decay of a V-particle,  
 $\theta^0 \rightarrow \pi^+ + \pi^-$  or  $\Lambda^0 \rightarrow \pi^- + p^+$ .



ZN-1194

Fig. 18. A V-particle created through the possible reaction,  
 $\pi^- + p^+ \rightarrow \theta^0 + \Lambda^0$ , and the decay of one of these V-particles.



ZN-1195

Fig. 19. A stereoscopic view of possible  $\pi$ -meson pair production,  
 $\pi^- + p^+ \rightarrow \pi^- + p^+ + \pi^+ + \pi^-$ .

## CHAPTER VII

### FUTURE DEVELOPMENTS

#### 1. General.

Because, until recently, all the work in the development of larger liquid hydrogen bubble chambers has apparently been done at the University of California Radiation Laboratory, this chapter discusses the work in progress at this institution. The four-inch chamber is being modified to make it a more effective and useful detector. Two larger chambers are being planned, based in many respects on the information gained from the operation of the four-inch model. The main objective, for reasons to be given later, is a chamber 50 inches long. As an intermediate step, a chamber ten inches in diameter is already under construction.

#### 2. The Four-inch Chamber.

The most important modification to the four-inch chamber is the addition of magnetic field coils to permit evaluation of the momenta of the particles. These coils are designed to be mounted around the chamber inside the vacuum jacket. The coils will create a pulsed field nearly uniform across the chamber with a maximum value of about ten kilogauss. The addition of the magnetic field required the replacement of the brass chamber with one of stainless steel construction to minimize heating due to eddy currents in the walls.

The expansion system is being modified by the addition of a quick-opening valve located just below the expansion cylinder. This valve is to be closed at the end of the recompression stroke, whereupon the piston in the expansion cylinder is immediately raised, creating a vacuum in the cylinder. When it is again desired to expand

the chamber, the valve will be opened, permitting the chamber to expand into the vacuum. This should provide a more rapid decrease in the chamber pressure. Preliminary tests using this new expansion system have been successful.

### 3. The Ten-inch Chamber.

The ten-inch chamber now under construction was designed to fit into an existing cloud chamber magnet. The chamber itself is to be ten inches in diameter and six inches deep. The magnet will create a field across the chamber of about ten kilogauss. A dc field is to be used to prevent excessive heating due to eddy currents.

This chamber is in many respects simply a larger version of the four-inch model, with some modifications dictated by the geometry of the existing magnet or considered desirable for other reasons. The chamber will be oriented with its glass windows horizontal. It will be illuminated from below by a system similar to the one already described for the four-inch chamber, except that the light will be incident on the edge of a circular lucite light diffuser which forms the bottom plate of the vacuum jacket. The vanes or shutter will form part of the liquid nitrogen thermal shield, minimizing one path of serious thermal radiation loss. Photography will be from above.

A valve will be substituted for the permanent restriction in the filling line. This arrangement will permit unobstructed flow during filling operations. The valve can later be throttled down to pass only enough hydrogen to replace that lost during operation. The gaseous hydrogen will be precooled in coils passing through both the liquid nitrogen and the liquid hydrogen flasks before it enters the chamber. A liquid nitrogen—liquid hydrogen coil will be wrapped around the chamber to permit precooling without introducing nitrogen into the

chamber.

At a later date the jacket can be adapted for chambers of different geometry such as a quarter-scale model of the 50-inch chamber discussed below.

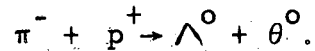
#### 4. The 50-inch Chamber.

The 50-inch chamber is a much more radical departure from the circular bubble chamber design. Its sensitive volume is to be 50 inches long by 20 inches wide by 20 inches deep. The beam will enter through one end on a path parallel to the long axis of the chamber. A large magnet is being designed to be built around this chamber to furnish a field of about 20 kilogauss. It is intended to include a refrigeration system as an integral part of the chamber system, to maintain the required temperature during operation.

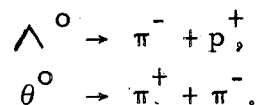
The design and construction of this chamber present many formidable but by no means hopeless problems. Some of these problems require considerable research into the little-explored field of the properties of materials at liquid hydrogen temperatures and the behavior of these materials as the temperature ranges from this value to room temperature. The large glass ports, 50 inches long, must be able to stand the rapid changes of pressure of the hydrogen in the chamber, and glass-to-metal seals must be developed that are effective throughout the entire temperature range, despite differences in the coefficients of thermal expansion between the two materials. An expansion mechanism is required which ensures rapid and equal reduction in the pressure over the entire volume of the chamber, and provision must be made for uniform illumination and photography of the entire sensitive region.

The dimensions of the chamber are somewhat arbitrary but,

nevertheless, have a firm foundation in theory. The chamber is being designed for use with the Bevatron, and one of the most important reactions to be investigated is



The  $\Lambda^{0}$  (lambda zero) is a hyperon and the  $\theta^{0}$  (theta zero) a K-particle, both of considerable interest to high-energy physicists. Both particles are neutral and thus will produce no ionization and create no tracks in the chamber. However, they have a relatively short lifetime and decay into charged, track-forming particles as follows:



It is not sufficient to have merely the point of decay in the chamber. One must have at least several inches of clearly defined tracks of the decay particles to determine the type of the original particle and its energy and direction. Fortunately, both the  $\Lambda^{0}$  and the  $\theta^{0}$  travel approximately the same distance during one lifetime, thus requiring approximately the same length of chamber for any given probability of seeing their decay products. Considering the distance a 6-Bev particle would travel during one lifetime and providing a reasonable length of chamber for the production of the  $\Lambda^{0}$  and  $\theta^{0}$  and for the tracks of the decay particles leads to a long dimension of roughly 50 inches. Similar considerations, with allowances for the spread of the incoming beam, point to a width and depth of about 20 inches.

##### 5. Data Compilation and Analysis.

A rapid means of analyzing and cataloging the accumulated data will be essential for use with such chambers. One logical method seems to be an electronic computer system similar to those presently used for computing the paths of rockets in flight. With this arrangement, an

operator would guide cross hairs along the tracks of the particle on the two stereoscopic views, and the computer would punch information on the path of the particle on cards. These cards could later be fed into machines for obtaining selected data.

## CHAPTER VIII

### ADVANTAGES AND CONCLUSIONS

#### 1. General.

Cosmic rays provide a natural source of high-energy elementary particles, but their extremely low intensity and wide energy distribution make the accumulation of information a long and tedious process. The need for a more rapid and accurate method of accumulation of basic information in that field of nuclear physics devoted to studying fundamental particles prompted the building of the high-energy accelerators.

A means of recording data as fast as they are produced by the Cosmotron-Bevatron type of accelerators, coupled with a systematic, accurate, and efficient means of analysis of the data, is mandatory if the money spent to build the large accelerators is to be justified (12). The accomplishment of both parts of this requirement has lagged for two different reasons. Efficient detection devices and techniques just have not been available; moreover, there is a serious lack of trained personnel to analyze the data.

The first real answer to the search for an efficient detector that also possessed the potentialities to make it a successful research tool when used in the high-intensity beams produced by the accelerators, came when Donald Glaser invented the bubble chamber in 1953.

Probably the best way to illustrate the superiorities of the bubble chamber is to compare its fundamental and inherent characteristics with those of other detection devices.

#### 2. Cloud Chambers.

Cloud chambers are of two types -- the expansion cloud chamber and the diffusion cloud chamber. These are visual detection devices,

and when placed in a magnetic field permit accurate measurements of particle momenta to be made. This can subsequently lead to the identification of the reaction observed. In many ways, the expansion-type chamber appears to be the better of the two for use with the accelerators. The tracks are clear and sharp, it has a thick sensitive active layer, and the fact that it is a pulsed detector makes it readily adaptable for use with the accelerators, which are also pulsed.

The diffusion chamber does not possess any of these advantages. Its tracks are fuzzy, its sensitive active layer is thin, and it is a continuously operating device. The fact that it operates continuously subjects it to serious background contamination from random ionizing radiation. The expansion chamber also is limited by this disadvantage, but to a lesser degree because it is a pulsed device and its sensitive time is short.

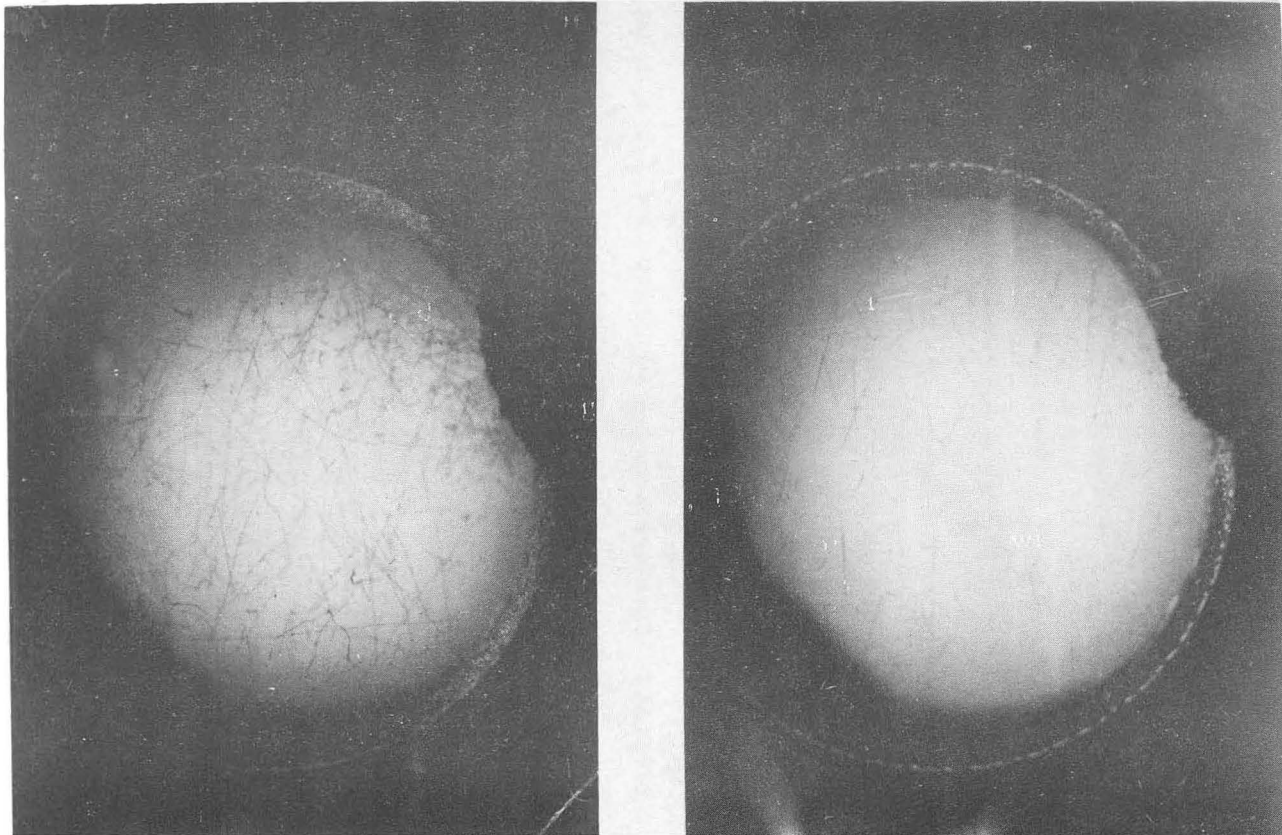
Neither chamber can take advantage of the high intensities available from the accelerators, and background contamination is not the only reason for this. To a first approximation, the number of nuclear events per unit length of track is directly proportional to the density of the material through which the ionizing particle is passing. Cloud chambers have therefore been designed to operate using high gas pressures to increase the density of the active material. For expansion chambers, use of high pressures is a serious disadvantage. At pressures around twenty atmospheres, recovery is so slow that the frequency of operation must be reduced to about one photograph every 15 minutes. This is usually so unacceptable that the diffusion chamber is preferred at these higher pressures in spite of all its other disadvantages. Diffusion chambers have an operating rate high enough to permit taking about two photographs per minute.

Finally, the diffusion chamber has another limitation, though it is not as troublesome in the expansion chamber. This is the fog produced in the active sensitive layer by  $\beta$ -rays from tritium contamination when high-pressure deuterium is used. Until an uncontaminated source of deuterium can be found, this gas will continue to be unsuitable for use in diffusion chambers.

On the other hand, the bubble chamber has all the advantages of the expansion chamber but is free of all the disadvantages mentioned above. The rate of operation of the bubble chamber can be as high as one cycle every three to five seconds. Secondly, and of extreme importance, the density of the liquid hydrogen is more than thirty times as great as that of the gas in a conventional pressure cloud chamber. And finally, by regulating the temperature of the liquid hydrogen, one can bias out the tracks of minimum-ionizing particles. Figures 20a and 20b illustrate this technique. Figure 20a was taken with a pulsed neutron source and with the chamber at  $27^{\circ}$  K. There is a dense background of electron tracks. The chamber temperature was then allowed to cool to  $26^{\circ}$  K and the experiment was repeated. Figure 20b shows the result: the electron tracks have been biased out and the recoil proton tracks can be easily identified. Deuterium has not yet been tried in a bubble chamber.

### 3. Nuclear Emulsions.

Nuclear emulsions, along with scintillation and Cerenkov counters, are commonly referred to as "solid detectors." The important role played by emulsions in the realm of high-energy physics cannot be overlooked, although they possess their own peculiar disadvantages. At first, emulsions were available only in thin layers, but improved methods soon followed which permitted the combining of many layers



ZN-1188

Fig. 20. An illustration of the biasing out of minimum-ionizing particles. (a)  $T = 27^{\circ}\text{K}$ . Note the dense electron background. (b)  $T = 26^{\circ}\text{K}$ . The electron tracks have been biased out and the recoil proton tracks can be easily identified.

of emulsions in one stack. Now the path of ionizing particles can be followed for relatively long distances. The technique of analysis is very exacting and tedious. Momenta are measured statistically by the small-angle scattering from the silver and bromine nuclei, whose higher atomic number, although increasing the Coulomb scattering, at the same time makes it impossible to utilize magnetic fields for the analysis of momenta.

Emulsions must be exposed for relatively long periods of time to give a high density of tracks if the method is to be economical. This consideration therefore introduces another objection, namely that the identification of related events is not possible.

In contrast, in the bubble chamber the creation and decay of two neutral particles, which for all practical purposes occur simultaneously, can be detected, and related, if the volume of hydrogen is sufficient. Worthy of consideration also is the negligible Coulomb scattering by hydrogen, due to its low atomic number, so that magnetic fields can be used to evaluate the momenta. This is done by simply measuring the curvature of the particle track.

#### 4. Counters.

Leaving the field of visual detectors, we next consider counters. Two disadvantages are most prominent-- that counters of efficient size have very poor spatial resolution, and that extraneous events are a serious problem in counter experiments. As has been pointed out previously, the details of any event are unlikely to be obscured in a bubble chamber. There is no basis for comparison, however, as far as time resolution is concerned. Scintillation and Cerenkov counters are far superior in this respect.

## 5. Conclusions.

In consideration of the above advantages and the results obtained with the somewhat hastily constructed four-inch chamber, we feel that liquid hydrogen bubble chambers will be one of the most effective and efficient detecting devices available to the high-energy nuclear physicist. They will be especially adaptable for use with the large accelerators of the Cosmotron-Bevatron type where the expansions can be synchronized with the pulsed beam. They should go far toward justifying the large amounts of money spent on the development and operation of these machines. (Their design may not, however, be easily adapted to cosmic-ray detection, as cosmic ray particles are unpredictable and not susceptible to control.)

Despite the tremendous difficulties certain to be encountered when working at liquid hydrogen temperatures, large chambers should prove not only possible but completely practical. These chambers, together with suitable analyzing and cataloging machines, should facilitate the rapid accumulation of large quantities of information of the most fundamental nature.

## BIBLIOGRAPHY

1. Glaser, D. A. SOME EFFECTS OF IONIZING RADIATION ON THE FORMATION OF BUBBLES IN LIQUIDS, *Physical Review*, 87, 665 (1952)
2. Glaser, D. A. A POSSIBLE "BUBBLE CHAMBER" FOR THE STUDY OF IONIZING EVENTS, *Physical Review*, 91, 496 (1953)
3. Gerritsen, A. N. IONIZATION BY ALPHA-PARTICLES IN LIQUIDS AT LOW TEMPERATURES, *Physica*, 14, 381 (1948)
4. Hildebrand, R. H. and Nagle, D. E. OPERATION OF A GLASER BUBBLE CHAMBER WITH LIQUID HYDROGEN, *Physical Review*, 92, 517 (1953)
5. Wood, J. G. BUBBLE TRACKS IN A HYDROGEN-FILLED GLASER CHAMBER, *Physical Review*, 94, 731 (1954)
6. Onnes, H. K. EXPRESSION OF THE EQUATION OF STATE OF GASES AND LIQUIDS BY MEANS OF SERIES, *Communications from the Physical Laboratory at the University of Leiden*, 71, 5 (1901) (Translated from: "Verslagen van de Afdeeling Natuurkunde der Kon. Akademie van Wetenschappen te Amsterdam", 29 Juni 1901, p 136-158)
7. Glaser, D. A. PROGRESS REPORT ON THE DEVELOPMENT OF BUBBLE CHAMBERS, *Nuovo cimento*, 11, Suppl. 2, 361 (1954)
8. Rayleigh, J. W. S. ON THE PRESSURE DEVELOPED IN A LIQUID DURING THE COLLAPSE OF A SPHERICAL CAVITY, *Philosophical Magazine*, 34, 94 (1917)
9. Plesset, M. S. and Zwick, S. A. THE GROWTH OF VAPOR BUBBLES IN SUPERHEATED LIQUIDS, *Journal of Applied Physics*, 25, 493 (1954)

10. Forster, H. K.  
and Zuber, N. GROWTH OF A VAPOR BUBBLE IN A  
SUPERHEATED LIQUID, Journal of  
Applied Physics, 25, 474 (1954)
11. de Brey, H.,  
Rinia, H., and FUNDAMENTALS FOR THE DEVELOP-  
van Weenen, F. L. MENT OF THE PHILIPS AIR ENGINE,  
Philips Technical Review, 9, 102 (1947)
12. Alvarez, L. W. THE BUBBLE CHAMBER PROGRAM AT  
UCRL, April 18, 1955 (unpublished)

## ALPHABETICAL AUTHOR LIST

Author	Bibliography Number
Alvarez, L. W.	12
de Brey, H.	11
Forster, H. K.	10
Gerritsen, A. N.	3
Glaser, D. A.	1, 2, 7
Hildebrand, R. H.	4
Nagle, D. E.	4
Onnes, H. K.	6
Plesset, M. S.	9
Rayleigh, J. W. S.	8
Rinia, H.	11
van Weenen, F. L.	11
Wood, J. G.	5
Zuber, N.	10
Zwick, S. A.	9